Geological Society, London, Special Publications Online First

Coastal structure, sea-level changes and vertical motion of the land in the Mediterranean

Marco Anzidei, Kurt Lambeck, Fabrizio Antonioli, Stefano Furlani, Giuseppe Mastronuzzi, Enrico Serpelloni and Gianfranco Vannucci

Geological Society, London, Special Publications, first published June 25, 2014; doi 10.1144/SP388.20

Coastal structure, sea-level changes and vertical motion of the land in the Mediterranean

MARCO ANZIDEI[1]*, KURT LAMBECK[2], FABRIZIO ANTONIOLI[3], STEFANO FURLANI[4], GIUSEPPE MASTRONUZZI[5], ENRICO SERPELLONI[1] & GIANFRANCO VANNUCCI[1]

[1]*Istituto Nazionale di Geofisica e Vulcanologia, Italy*

[2]*Research School of Earth Sciences, Australian National University, Canberra, Australia*

[3]*ENEA Special Project Global Change, S. Maria di Galeria, Rome, Italy*

[4]*DMG, Dipartimento di Matematica e Geoscienze, Università di Trieste, Italy*

[5]*Dipartimento di Scienze della Terra e Geoambientali, Università degli Studi 'Aldo Moro', Bari, Italy*

**Corresponding author (e-mail: marco.anzidei@ingv.it)*

Abstract: The Mediterranean basin is an important area of the Earth for studying the interplay between geodynamic processes and landscape evolution affected by tectonic, glacio-hydro-isostatic and eustatic factors. We focus on determining vertical deformations and relative sea-level change of the coastal zone utilizing geological, archaeological, historical and instrumental data, and modelling. For deformation determinations on recent decadal to centennial time scales, seismic strain analysis based on about 6000 focal mechanisms, surface deformation analysis based on some 850 continuous GPS stations, and 57 tide gauge records were used. Utilizing data from tectonically stable areas, reference surfaces were established to separate tectonic and climate (eustatic) signals throughout the basin for the last 20 000 years. Predominant Holocene subsidence (west coast of Italy, northern Adriatic sea, most of Greece and Turkey are areas at risk of flooding owing to relative sea-level rise), uplift (local areas in southwestern Italy and southern Greece) or stability (northwestern and central western Mediterranean and Levant area) were determined. Superimposed on the long trends, the coasts are also impacted by sudden extreme events such as recurring large storms and numerous, but unpredictable tsunamis caused by the high seismicity of parts of the basins.

Supplementary material: A table of locations and timings of the largest tsunamis in the Mediterranean during the last 5660 years BP is available at http://www.geolsoc.org.uk/SUP18757.

The complex morphological and structural setting of the Mediterranean region is the result of the evolution of deep basins and arcuate fault-and-thrust belts that originated during the long-lasting convergence between the major Africa and Eurasia plates running along an east–west boundary (Dewey *et al.* 1973; Le Pichon *et al.*1988; Fig. 1). This convergence has been active since the Late Cretaceous and currently is of the order of few millimetres per year (Serpelloni *et al.* 2007). In consequence, the region is characterized by narrow seismic belts as well as a broad zone of seismicity and deformation that characterizes the Alpine belt, indicating a complex pattern of crustal stress and strain fields across these zones (Rebai *et al.* 1992; Vannucci *et al.* 2004). The recent earthquake distribution also identifies the boundaries of minor plates whose interiors appear to be largely aseismic (Serpelloni *et al.* 2007, 2010). About 50 subaerial and submarine volcanoes are active or quiescent in this region (http://www.volcano.si.edu/). Under the combination of the seismicity and volcanism the coastal regions are often struck by destructive tsunami (Guidoboni 1994; Guidoboni & Comastri 2007).

With its crustal dynamics, volcanism and associated coastal processes, and with a comparatively long record of archaeological, historical and instrumental evidence of their consequences, the Mediterranean basin provides valuable data for studying the underlying processes. Elements that are important in quantifying these processes include the rates of deformation, the horizontal components of which are usually better constrained by observations than the vertical components, geological observations of the latter being limited to the change of land surfaces relative to sea level which itself is time and spatially variable. Hence we have focused on this component in this paper, including its

From: Martini, I. P. & Wanless, H. R. (eds) *Sedimentary Coastal Zones from High to Low Latitudes: Similarities and Differences*. Geological Society, London, Special Publications, **388**, http://dx.doi.org/10.1144/SP388.20

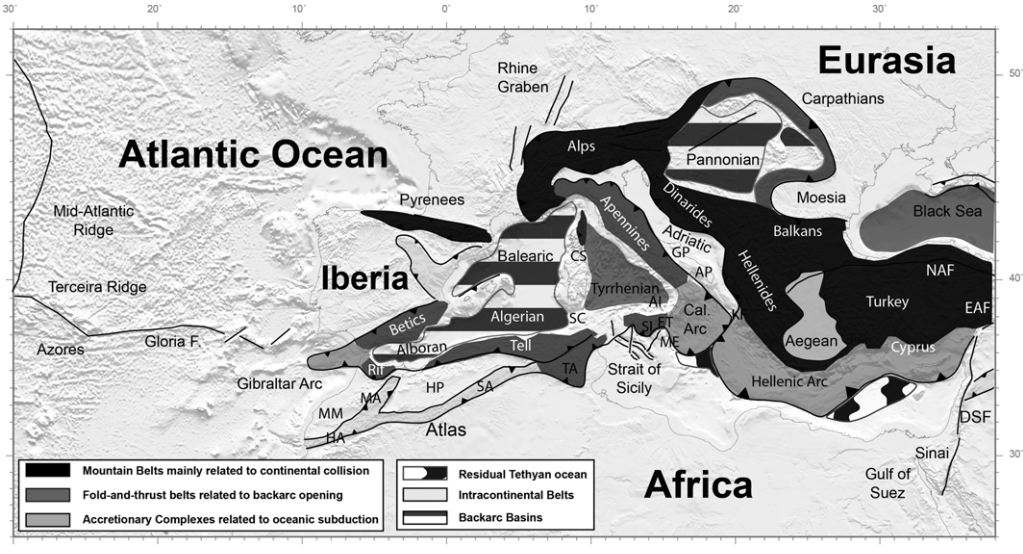

Fig. 1. Simplified tectonic map of the Mediterranean region. HA, High Atlas; MM, Moroccan Meseta; MA, Middle Atlas; SA, Saharian Atlas; TA, Tunisian Atlas; HP, High Plateau; SC, Sardinia Channel; ME, Malta Escarpment; SI, Sicily; AI, Aeolian Islands; ET, Mount Etna; PP, Pelagian Plateau; CS, Corsica–Sardinia block; AP, Apulian block; GP, Gargano Promontory; KF, Kephallinia fault zone (modified from Serpelloni *et al.* 2007).

separation from changes in sea level itself. Additionally, the Mediterranean basin has been inhabited by ancient populations since Palaeolithic times and the archaeological traces of past civilizations can still be found along its coasts and submerged. Knowing the movements of the land and sea surfaces through time can provide important insight into the uses of these structures as well as a guide to the exploration for submerged sites.

The Mediterranean basin has been shaped by geological processes over many millions of years, but we focus here on the geological history of the past 120 000–130 000 years corresponding to the time interval from the Last Interglacial (Marine Isotope Stage 5e) to the Present. Spatially, we focus on the coastal zone of this basin. Geological processes remain a significant factor in the basin evolution, but climate-related processes also play a significant role. The primary factor affecting the coastal evolution in this interval is the sea-level change driven by the growth and decay of the large ice sheets culminating in the Last Glacial Maximum (LGM) about 20 000 years ago. This results not only in a global change in sea level, the eustatic component, but also in the associated isostatic effect as the Earth's gravity, shape and rotation respond to the changing surface loads of ice and water. Combined, the eustatic and glacio-hydro-isostatic contributions produce the principal basin-wide-scale change in relative sea level throughout the Pleistocene and Holocene (Lambeck *et al.* 2004*a*; Lambeck & Purcell 2005). Observational evidence and numerical analysis developed during the past two decades of these effects has led to predictive models of this changing shoreline geometry and land elevations. These provide a reference for inferring tectonic rates of uplift and subsidence of the basin margin, reflecting the active tectonic and volcanic regimes of the region (Flemming & Webb 1986), and modulate the sea level from a largely predictive function to a much more spatially and temporally variable predictive function.

We review some of the evidence and analysis results for the relative sea-level change – the disposition of the sea surface relative to the land surface – using a range of geological, archaeological and instrumental records. The first of these, the geological data, are from two main periods: the Last Interglacial (MIS 5e) and the Holocene. The Last Interglacial was a period when climate conditions and sea levels were similar to those of the Late Holocene such that shoreline elevations of this earlier period should lie within a few metres of present sea level. Observations of MIS 5e shorelines therefore provide a first approximation estimate of the total land uplift or subsidence over the past *c.* 125 000 years. The geological record becomes more complete for the post LGM period, particularly for the Holocene, and it is these data that provide the constraints on the eustatic–isostatic models for the region as well as estimates of vertical tectonic rates – from the discrepancies between

observational and model values – on time scales of 1000–10 000 years. The archaeological data used here concentrate on the Roman Epoch harbour and fish tank structures and a growing body of data is providing a good constraint on sea levels at *c.* 2000 years ago and on tectonic rates since then. The high precision instrumental record extending back about 100 years, covers a period when climate-related contributions were relatively more significant than those of tectonic and isostatic factors. The comparison of this detailed information on the relative contribution of the various factors with existing longer-period, pre-instrumental, records provides a basis for separating out the effects of the different processes.

The geological evidence for sea-level change does not necessarily discriminate between the long-term trends and short-duration episodic events such as storm surges and tsunami. Hence we have also examined the nature and effects of these episodic events and their historical record. Of the 300 extreme events recognized across the Mediterranean basin, only 15 can be confidentially attributed to tsunamis.

Direct information on crustal vertical movements comes from instrumental data. We consider two classes of such information: (a) seismic strain analysis based on about 6000 focal mechanisms across the Mediterranean region; and (b) surface deformation analysis based on some 850 continuous GPS stations. The former dataset spans about 130 years with more accurate, extensive data for the last *c.* 30 and a more heterogeneous, smaller dataset extending back the information to about 100 years before present. The surface-deformation records span intervals from the last 2.4 to 14 years with most of the sites located on the northern side of the Mediterranean basin. In keeping with the focus on the coastal zone, we present here only the results for locations within 20 km of the coast.

While the results of the instrumental data analyses are provisional, the trends and magnitudes of the vertical rates are similar for the two distinctly different, independent analyses. The results of the sea-level data consolidate the validity of the methodologies adopted and emphasize the value of the integrated approach.

Geological setting

In recent decades several seismotectonic syntheses have been proposed for the Mediterranean basin to describe the present-time tectonics and kinematics of this region (Jackson & McKenzie 1988; Westaway 1990; Kiratzi & Papazachos 1995; Vannucci *et al.* 2004; Serpelloni *et al.* 2007). Of the several active tectonic structures in the region, the Hellenic Arc system is the largest and the most active, causing a broad deformation in the eastern Mediterranean, and is responsible for most of the largest earthquakes. In the central part, the subduction of the Calabrian Arc and the volcanism associated with the Aeolian Islands are the most important active features that control the kinematics of this area (Hollenstein *et al.* 2003; Serpelloni *et al.* 2010). In this tectonic framework, geological and geodynamic processes acting on different spatial scales are causing horizontal and vertical motion of the Earth surface that involves the coastal areas (Anzidei *et al.* 2011*a*, *b*). The largest present crustal movements occur at rates up to 30–40 mm a^{-1} in horizontal directions for parts of the eastern (Aegean) Mediterranean, but rarely exceed 1–2.5 mm a^{-1} in the vertical (Lambeck 1995; Ferranti *et al.* 2006; 2010; Serpelloni *et al.* 2006, 2007). When extrapolated back in time, their cumulative effects, assuming that they have continued at similar rates over thousands to millions of years, have produced dramatic changes of the plate margins, mountain chains and coastal environments.

The largest critical effect of these movements occurred around 6 Ma BP, with the closure of Gibraltar Strait, blocking the entrance of Atlantic waters into the Mediterranean basin and leading to the drying out of most of the enclosed sea. This is the Messinian Salinity Crisis (Hsu *et al.* 1973; Garcia-Castellanos *et al.* 2009) during which the Mediterranean Sea lost most of its water through evaporation and its level dropped more than 1300 m below the current level (Fig. 2). Thick sequences of evaporites were deposited in the hyper-saline abyssal plains and are now exposed, for example, in salt mines in Sicily (Figs 3 & 4a).

The Messinian crisis ended about 5.3 million years ago, when the marine gateway to the Atlantic was restored (Duggen *et al.* 2003). Since then, the evolution of the Mediterranean coastal zone has been governed by the interaction between tectonics and climate-induced sea-level oscillations, as shown by the stratigraphic sequences in subsiding coastal plains, shallow shelves or in drowned littoral caves that provide information on Pleistocene sea-level oscillations (Van Andel 1989; Antonioli *et al.* 2004*a*; Dorale *et al.* 2010). An example of the palaeoshoreline reconstruction for more recent periods is given by Furlani *et al.* (2013), who examined the area between southern Sicily and northern Africa from the LGM to the Present. There, Malta island was connected to the European mainland via Sicily and only between 14.5 and 13.8 Ka cal BP, when local sea level was about 100–90 m lower than today, did Malta become an island.

Presently, flights of marine terraces either submerged or on emerging coastlines preserve the

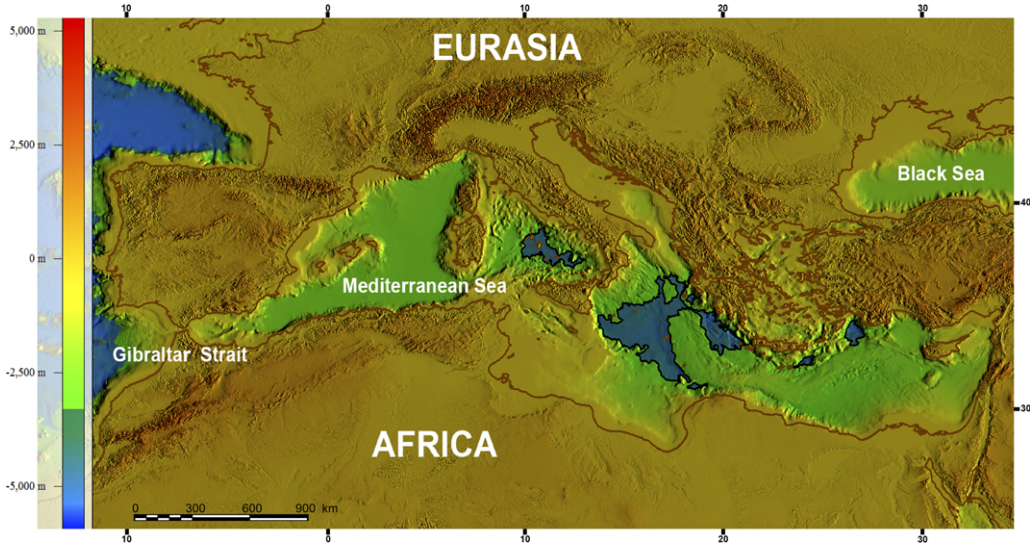

Fig. 2. Palaeogeographic reconstruction of the Mediterranean coastlines during the Messinian salinity crisis, about 6 Ma BP. The reconstruction does not take into account the effects of erosion and tectonic displacement, and is therefore only indicative. Note the closure of the Gibraltar Strait, the separation of the Black Sea from the Mediterranean Sea, the continental link between Sicily and Africa and the drying of the Adriatic Sea. In blue is the estimated Messinian extension of the Mediterranean basin (coastlines are in black). Map is based on Shuttle Radar Topographic Mission (SRTM) data for surface topography and General Bathymetric Chart of the Oceans (GEBCO) data for bathymetry. In brown are the current coastlines. No allowance has been made for the isostatic rebound of the crust in response to the water unloading.

signatures of sea-level highstands (Ferranti *et al.* 2006, 2010; Rovere *et al.* 2011; Romagnoli 2013). These have been widely used to estimate long-term vertical land movements (Keraudren & Sorel 1987; Goy & Zazo 1988; Dumas *et al.* 1993; Zazo *et al.* 1999; Carobene & Dai Pra 2003; Rodriguez-Vidal *et al.* 2004; Ulug *et al.* 2005). These surfaces are usually assumed to have formed during successive interglacials in an uplifting environment, but in most instances it is only the Last Interglacial shoreline of *c.* 125 000 years ago that can be securely dated.

Geodynamic analysis

Seismicity and current seismic strain

The Mediterranean seismicity marks the Africa–Eurasia plate boundary from the Azores Islands to the Arabic plate along seismic belts and complex patterns of crustal stress and strain fields (Jackson & McKenzie 1988; Westaway 1990, 1992; Rebai *et al.* 1992; Pondrelli *et al.* 1995; Serpelloni *et al.* 2007). Earthquakes and tsunami across this area (Figs 5 & 13) (Vannucci *et al.* 2004; Vannucci & Gasperini 2004; Pirazzoli *et al.* 1994, 1996*a*, *b*; Stiros 2001, 2010; Mastronuzzi & Sansò 2002, 2012; Shaw *et al.* 2008; Mastronuzzi *et al.* 2013*a*) have resulted in hundreds of thousands of human victims in the last few centuries alone and since historical times have played a fundamental role in the development of civilization and landscape changes in the region (Guidoboni 1994; Guidoboni & Comastri 2007).

Traditionally, the estimation of deformation from seismic data has focused on the horizontal component of seismic deformation, but, with the aim of improving the current strain maps for the Mediterranean region and of estimating longer-term vertical tectonic rates, we have estimated the seismic deformation trends along the vertical from seismic data using the Moment Tensor Summation (MTS) technique (Kostrov 1974). This method provides a quantitative evaluation of the average strain of a number (N) of earthquakes within a rock volume (V) (the rock layer characterized by a length, width and thickness of the seismogenic zone). The Kostrov (1974) methodology corresponds to the basic equation:

$$\bar{\varepsilon}_{ij} = \frac{1}{2\mu V}\sum_{k=1}^{N} M_{ij}^{k} \ldots \qquad (1)$$

where $\bar{\varepsilon}_{ij}$ is the seismic strain, μ the shear modulus ($=3 \times 10\ \mathrm{N\ m^{-2}}$), and the sum of the moment

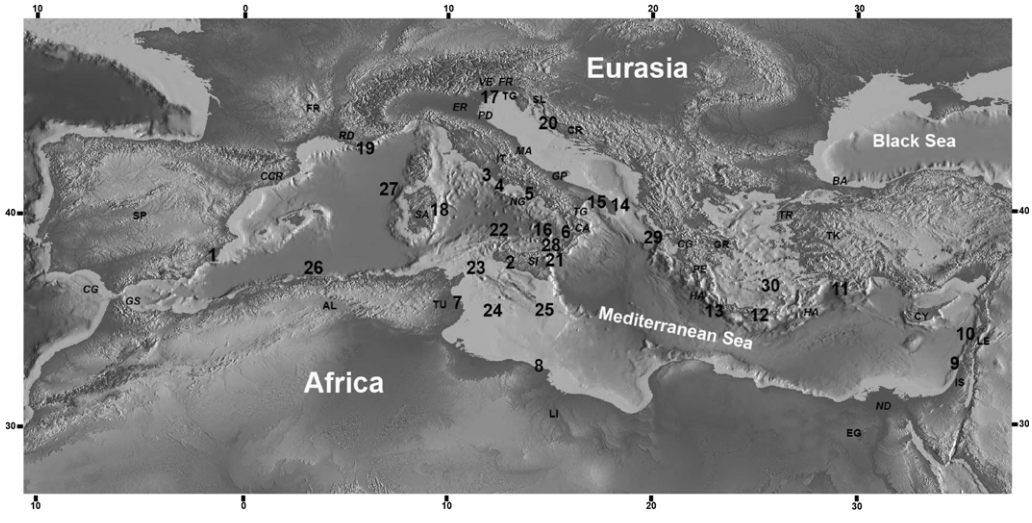

Fig. 3. Map with the location of the sites described in this paper. 1, Alicante (Spain); 2, Realmonte (Sicily, Italy); 3, Tyrrhenian coast near Rome (Latium, Italy); 4, Torre Astura (Latium, Italy); 5, Baia (Campania, Italy); 6, Briatico (Calabria, Italy); 7, Mraissa (Tunisia); 8, Leptis Magna (Libya); 9, Cesarea Marittima (Israel); 10, Sidon and Tyre (Lebanon); 11, the coast of near Fethye (Turkey); 12, Ierapetra, (Crete, Greece); 13, Phalasarna (Crete, Greece); 14, Otranto (Apulia, Italy); 15, Taranto Gulf (Apulia, Italy); 16, Basiluzzo Island (Aeolian Islands, Italy); 17, Venice (Italy); 18, Orosei Gulf (Sardinia, Italy); 19, Marseille (France); 20, coast of Croatia; 21, Taormina and Augusta (Sicily, Italy); 22, Ustica island (Italy); 23, Pantelleria Island (Sicily, Italy); 24, Lampedusa Island (Sicily, Italy); 25, Malta island; 26, Le Figuer (Algeria); 27, Capo Caccia (Sardinia, Italy); 28, Messina Straits with the towns of Reggio Calabria (Calabria, Italy) and Messina (Sicily, Italy); 29, Lefkada Island (Greece); 30, Santorini Island (Greece). AL, Algeria; BA, Bosphorus area; CA, Calabria; CCG, Catalan Coastal Range; CG, Corinth Gulf; CR, Croatia; CY, Cyprus; EG, Egypt; ER, Emilia Romagna; FR, France; FR, Friuli Region; GC, Gulf of Cadiz; GP, Gargano Promontory; GR, Greece; GS, Strait of Gibraltar; HA, Hellenic Arc; IS, Israel; LE, Lebanon; LI, Libya; MA, Marche–Abruzzi region; ND, Nile Delta; PD, Padana Plain; PE, Peloponnesus; RD, Rhone Delta; SA, Sardinia; SL, Slovenia; SP, Spain; TG, Taranto Gulf; TK, Turkey; TR, Troy; TU, Tunisia; SI, Sicily; VE, Veneto Region.

tensor elements M_{ij} is taken for $k = 1, \ldots, N$ earthquakes.

The coseismic deformation (Pondrelli *et al.* 1995; Pondrelli 1999), evaluated in three dimensions and integrated over time, allows the average vertical strain rate (VSR, v_z^z) to be estimated by using the relation of Jackson & McKenzie (1988):

$$v_z^z = \frac{1}{2\mu t a} \sum_{k=1}^{N} M_{33}^k \cdots \qquad (2)$$

where t is the time period on which earthquakes occurred, and a is the area on the Earth surface of the analysed seismogenic volume.

We applied the MTS technique (eqn (1)) and the VSR formula (eqn (2)) over all focal mechanisms (FMs) available in the Mediterranean region (20°W–45°E in longitude, 25–51°N in latitude). In this area the convergence between the African and Eurasian plates is accommodated across rather localized deformation zones and characterized by the alternation of various tectonic styles in narrow spaces. The dataset (Table 1) includes (a) the Global Centroid Moment Tensor (GCMT, Pondrelli *et al.* 2004, 2006, 2007; Ekström *et al.* 2005, http://www.globalcmt.org; (2) the National Earthquake Information Center of the US Geological Survey (NEIC/USGS; http://neic.usgs.gov/neis/sopar); (c) the European–Mediterranean RCMT Catalogue of the Istituto Nazionale di Geofisica e Vulcanologia (INGV; RCMT/INGV; Pondrelli *et al.* 2004, 2006, 2007); (d) the Time Domain Moment Tensor Catalogue of the INGV (TDMT/INGV; Scognamiglio *et al.* 2009, http://cnt.rm.ingv.it/tdmt.html); (e) the moment tensor datasets of the Eidgenössische Technische Hochschule of Zurich (ETHZ; Braunmiller *et al.* 2002, http://www.seismo.ethz.ch/prod/tensors/); (f) the Moment Tensor Catalogue of the Instituto Andaluz de Geofísica of Granada University (IAGG; Stich *et al.* 2006, http://www.ugr.es/~iag/tensor/mtc.html); and (g) the Seismic Moment Tensor Catalogue of the Instituto Geografico National of Madrid (IGNM; Rueda & Mezcua 2005, http://www.ign.es/ign/layout/sismo.do). The above-mentioned

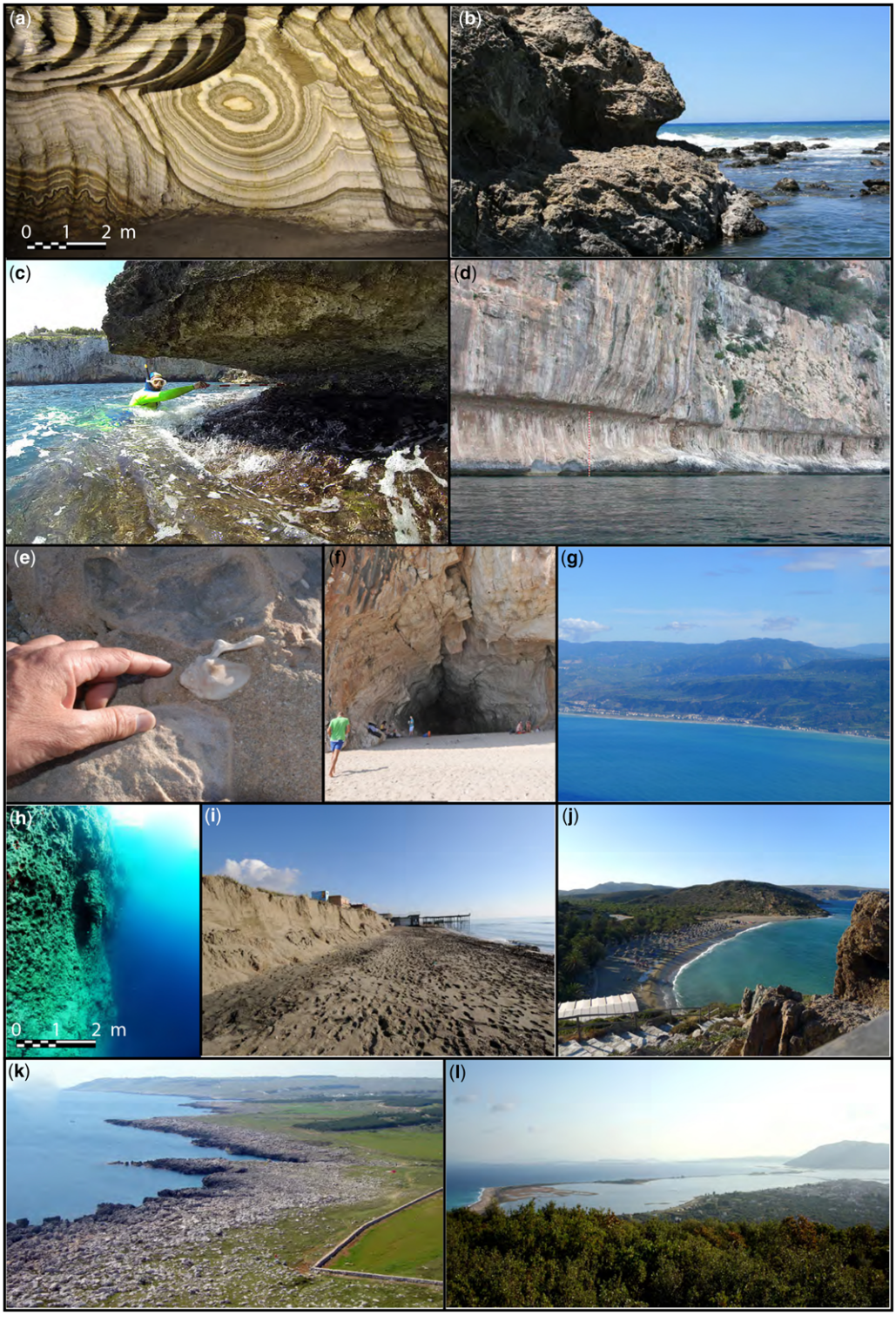

datasets cover a time span of about 30 years, although several regional catalogues are not complete for lower magnitudes, and durations and the data collected are scattered in time and magnitude. To extend the time coverage back in time to about 100 years before present we have added (h) the EMMA database (Vannucci & Gasperini 2004; Vannucci *et al.* 2004) – a heterogeneous collection of FMs (mainly first-pulses) published in the literature from several studies – even though it is not complete and homogeneous in time, magnitude and area coverage. Owing to the heterogeneous collection of all the data and to the use of different catalogues, we applied different criteria to determine the preferred solution when more than one focal mechanism is available from different sources for the same event. The complete dataset of the investigated area includes about 6000 preferred FMs and allows detailed analyses in space and time by computing the cumulative coseismic strain. In particular we estimated the tectonic style by using the MTS technique and the VSR formula over crustal volumes derived from a regular mesh with step of 0.5°, in both latitude and longitude in a 35 km-thick seismogenic layer (Serpelloni *et al.* 2007).

The resulting tectonic style for different areas – that is, the summation of Moment Tensors (FMsum) – can be mapped as plot of 'beach balls' or deformation axes. We have chosen to use the Frohlich Ternary Diagram (FTD; Frohlich 1992) where the corners represent the main tectonic styles: compressive, strike-slip and extensional (Fig. 6). Each vertex of the FTD is assigned a red–green–blue (RGB) colour function: in red a pure compressive regime, in green a strike-slip regime and in blue an extensional regime (insert in Fig. 6). Each of the three colours varies in the numerical range between 0 and 255 starting from each vertex towards the centroid of the FTD. Along the medians of the triangle the value is the maximum of the 0–255 colour scale, while in the segment under the centroid the value linearly trends to the minimum (0). For each volume of the grid used for subdividing the working area, the corresponding FM sum is located in a point of the FTD, which represents the FMsum and the corresponding tectonic style as an RGB colour.

On the same grids and dataset of FMs used to identify the prevailing tectonic styles, we also computed the vector of VSR (up or down) that reveals well-defined regions of negative and positive motion (Fig. 7). Of these, the former are areas characterized by extensional regimes and the latter are areas of compressive tectonic style, corresponding, respectively, to trailing-edge and collision-type coasts (Inman & Nordstrom 1971). The amount of vertical motion is mostly within the range between -0.04 and 0.04 mm a^{-1}, although several grid cells show positive (up-motion) and negative (down-motion) values up to -1.0 and 1.0 mm a^{-1}.

Geodetic deformations from GPS data

The vertical component of the Earth's surface velocity field is important for constraining deep-seated geodynamics, active tectonics, and magmatic and hydrologic processes, and to determine relative sea-level changes along the coasts, among other applications. However, although for more than a decade the Global Positioning System (GPS) has been widely used for measuring horizontal deformations with excellent precisions even in slowly deforming regions, such as the Mediterranean and its mountain belts (Serpelloni *et al.* 2002, 2005, 2007; Bennet *et al.* 2012; Nocquet 2012), our knowledge of vertical movements in this same area is still elusive because vertical GPS velocities are more difficult to measure than horizontal ones for several reasons: primarily, the precision of vertical GPS positions is typically about 3–5 times lower than the horizontal and vertical velocities, in a global reference frame, are usually an order of magnitude smaller than the horizontal ones, in addition to the geometric weaknesses in the height component of continuous GPS (cGPS) (Altamimi *et al.* 2011).

Despite the limitations, in this section we have used a subset of a recently published geodetic vertical velocity solution, based on cGPS stations from across the Euro-Mediterranean region (Serpelloni *et al.* 2013). Figure 8 shows the present-day vertical

Fig. 4. Examples of coastal morphology and geology. (**a**) Salt layers of Messinan age in the Realmonte mine (Sicily, Italy). (**b**) uplifted rocky coast near Phalasarna, Crete (Greece). (**c**) Present marine notch in Apulia (Italy). (**d**) Tidal notches in Sardinia at Cala Gonone (Italy). (**e**) *Persististrombus latus* (Gmelin) of MIS 5e age along the coast of Tunisia. (**f**) Coastal caves along the coast of Sardinia at Cala Gonone (Italy). (**g**) Uplifted marine terraces in Calabria (Italy). (**h**) Submerged stalactite (unknown age) along the coast of Fethye (Turkey). (**i**) Eroded sandy beaches near Rome (Italy). (**j**) Indented coastlines in Greece. (**k**) Mega boulder berm at Torre Sant'Emiliano (Apulia, Italy). This boulder accumulation is characterized by two different crests stretching for about 2.5 km and up to 200 m inland at an elevation of about 13 m above current mean sea level. It is composed of thousands of boulders weighing up to 70 t each. Some show bioconcrection of *Lithophyllum licheinodes*. ^{14}C data and archaeological evidences from below these boulders permit correlation of the deposition with the tsunami of 20 February 1743. (**l**) The Gyrapetra tsunami chevron into the Lefkada lagoon (Ionian Islands, Greece) as seen from the road to Tsoukalades near the Faneromenis Monastery.

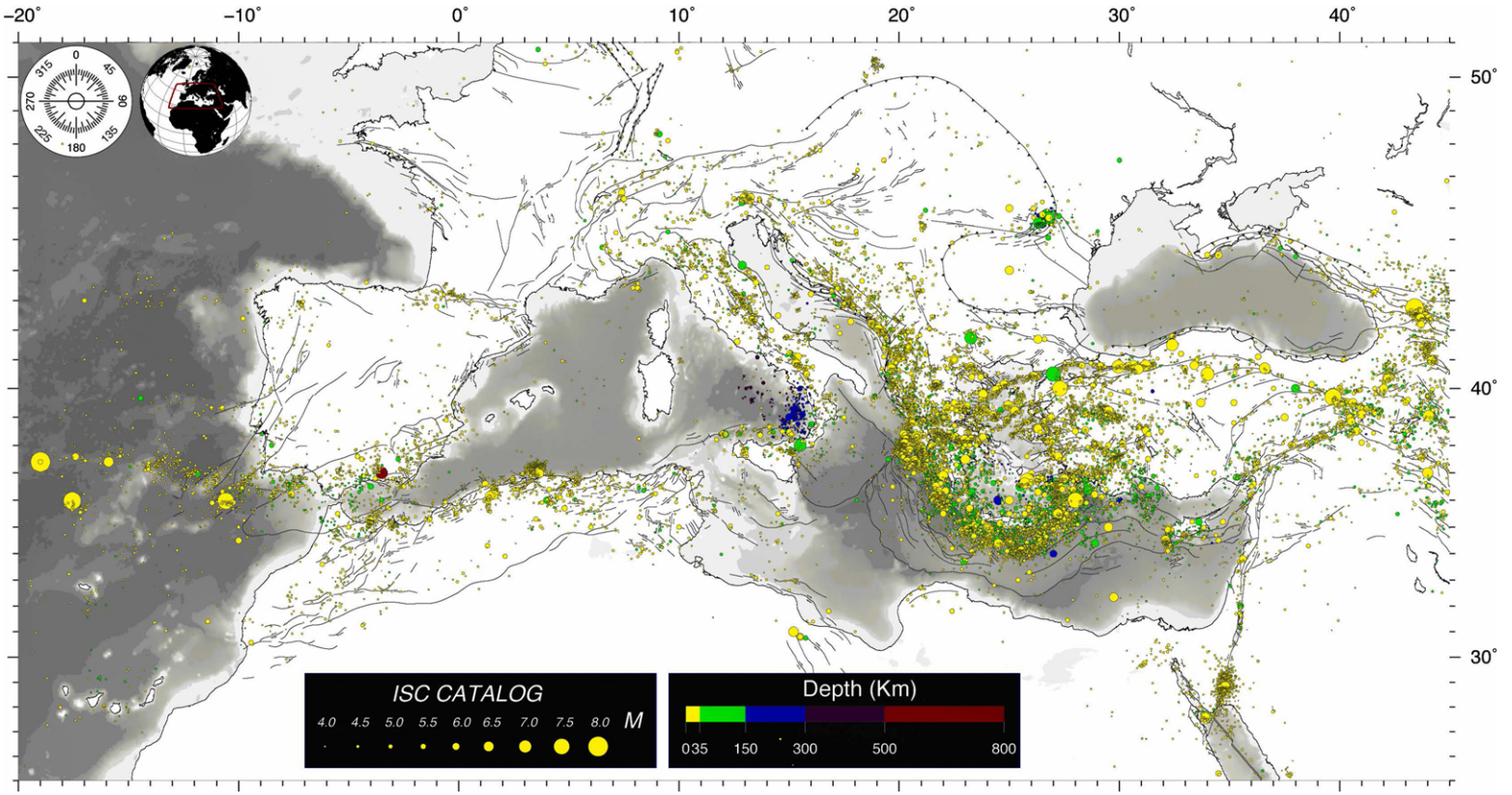

Fig. 5. Seismicity ($M > 4$) of the Mediterranean basin in the time span 1900–2012 from the International Seismological Centre, on-line catalogue (ISC 2001, http://www.isc.ac.uk/).

Table 1. *The seismic catalogue data base used in this study*

Catalogue	Time Span	Magnitude
GCMT	1976–2013	$M \geq 4.3$
NEIC/USGS	1980–2010	$M \geq 5.0$
RCMT/INGV	1976–2013	$M \geq 3.9$
TDMT/INGV	2004–2013	$M \geq 2.8$
ETHZ	1999–2006	$M \geq 2.8$
IAGG	1984–2005	$M \geq 3.3$
INGM	2002–2012	$M \geq 3.3$
EMMA	1905–2010	$M \geq 0.7$

Time span and magnitude refer to data available in the area of Figure 5.

velocities of cGPS stations located at distances less than 20 km from the coastlines of the Mediterranean basin. These velocities are part of a broader geodetic solution that includes more than 850 cGPS stations. The number and density of stations are higher for the northern side of the Mediterranean basin, where most of the cGPS networks have been in operation for many years. The three-dimensional geodetic velocities have been estimated from the analysis of 2.5–14 years long-position time-series in the January 1998–March 2011 time interval. Velocities and uncertainties have been obtained adopting a three-step approach, as in Serpelloni *et al.* (2007, 2010), including (a) the GPS phase data reduction using GAMIT software (Herring *et al.* 2010), (b) the combination of solutions and reference frame definition and (c) the time-series analysis. The reference frame has been obtained by minimizing coordinates and velocities of the IGS global core stations, while estimating a seven-parameter transformation with respect to the IGS realization of the ITRF2008 reference frame (Altamimi *et al.* 2011). Additional details on the data analysis are reported in Serpelloni *et al.* (2013). With respect to previous work, the spatially correlated common mode errors (Wdowinski *et al.* 1997) and the stochastic noise contents in the displacement data have been analysed with the goal of improving the signal-to-noise ratio and estimating uncertainties accounting for coloured noise in the data. Spatial filtering of position time-series obtained from the application of a principal component analysis (Dong *et al.* 2002, 2006) yielded a significant gain in the signal-to-noise ratio, with a reduction of *c.* 30% in the weighted root mean square of the vertical time-series. A maximum likelihood estimation method has been used to estimate the stochastic noise content in the filtered time-series and the average spectral index, *c.* 0.7, is suggestive of a power-law plus white noise stochastic error model. The application of a space–time filter, with removal of a common mode error in the displacement data, further improves the precisions of

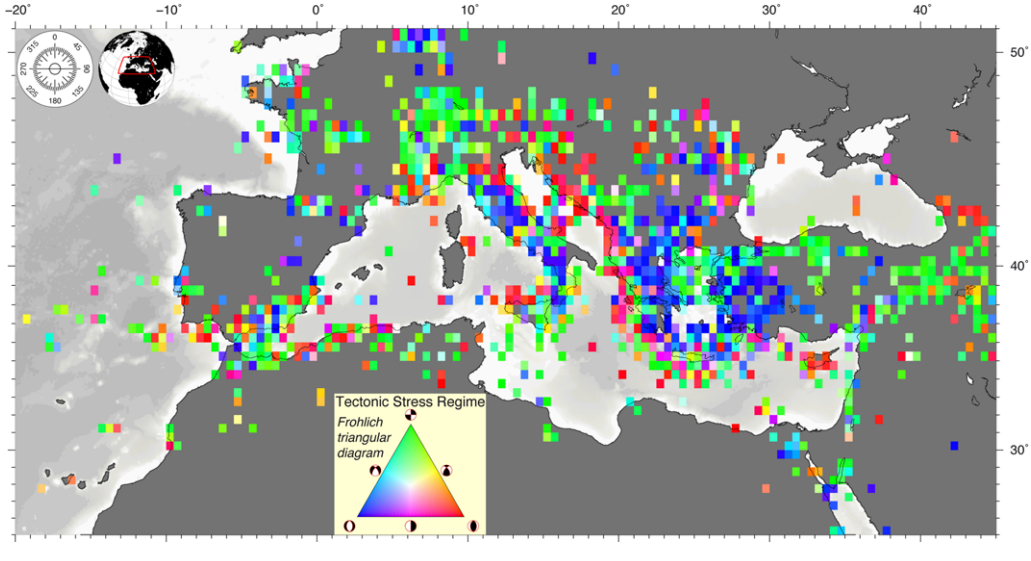

Fig. 6. Tectonic regimes in the Mediterranean computed using the Moment Tensor Summation technique from seismic data (Kostrov 1974). The tectonic style is represented by the red–green–blue colour palette of the Frohlich ternary diagram (FTD, Frohlich 1992; see text for details). Focal mechanisms (FMs) within the seismogenic thickness of 35 km and regular grids with mesh of 1° have been used. The corners of the FTD show compressional, strike-slip and extensional movements of the Earth's crust.

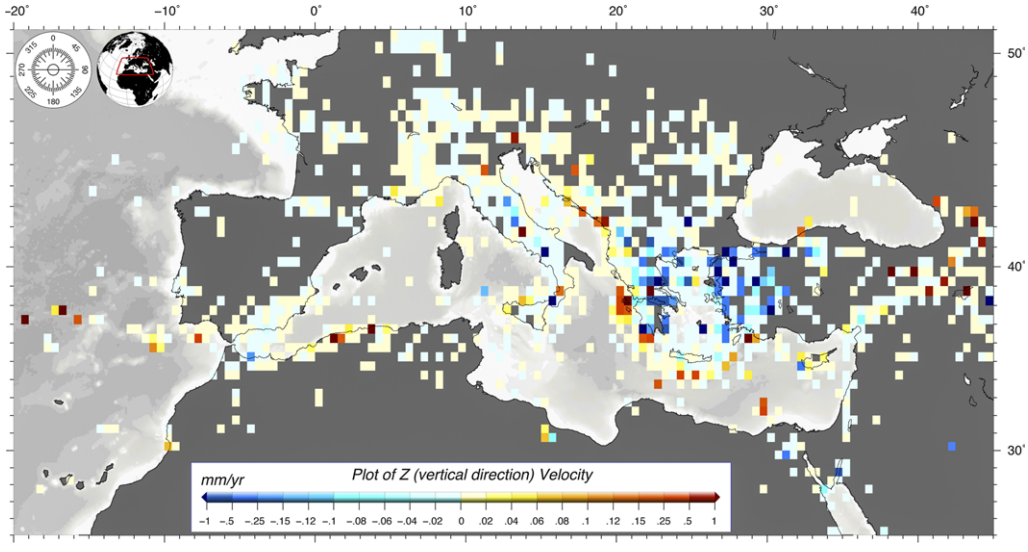

Fig. 7. Vertical strain rates computed from focal mechanisms for each crustal volume (see Fig. 5 and text for details).

the vertical GPS velocity estimates with uncertainties estimated from filtered time-series on average *c.* 40% smaller than uncertainties from unfiltered time series. Vertical velocity uncertainties are in the range of 0.1–2 mm a^{-1}, with a mean velocity error of 0.39 and a standard deviation of 0.29 mm a^{-1}. Some 95% of the GPS stations show a velocity uncertainty lower than 0.95 mm a^{-1}. Figure 8 shows the smoothed horizontal velocity field obtained from a interpolation of the discrete horizontal velocities given with respect to the Eurasian frame.

The limited coverage of cGPS sites in southern Europe and their almost total absence in northern Africa lead to only a partial picture of the current crustal motion across the region as a whole. Nevertheless, the spatial variability of these velocities highlights the different tectonic and volcanic environments that characterize the Mediterranean region. Along the coast of southern Iberia most of the GPS stations display subsiding behaviour, with the exception of three sites near Alicante that show small uplift (at rates less than 1 mm a^{-1}) in agreement with levelling data (Giménez *et al.* 2009). Subsidence rates are faster, at about −2 mm a^{-1}, near the Gulf of Cadiz and then decrease northeastward (*c.* 1 mm a^{-1}) along the coasts of the Catalan Coastal Range. The coasts of southern France and in the Gulf of Genoa display vertical velocities close to zero. In northern Tuscany, with the exclusion of a few sites, the predominant signal is subsidence at rates that increase toward the south at about −2 mm a^{-1}. In central Italy, along the coasts of the Lazio–Abruzzi region, the evidence points to near zero movement or a small uplift at <1 mm a^{-1}. South of this area, along the coasts of Campania, subsidence is predominant and a few sites in the volcanic district of the gulf of Naples show rates up to about −8 mm a^{-1}.

In southern Italy, subsiding movements are recorded by some stations located along the Tyrrhenian coasts of Calabria, while the Ionian coast null or slow uplift rates are occurring at *c.* 1 mm a^{-1}. The volcanic arc of the Aeolian Islands, in the southern Tyrrhenian Sea, is undergoing rapid subsidence at rates up to −10 mm a^{-1}. The coasts of northern Sicily and the island of Ustica (located west of the Aeolian Islands) appear stable or uplifting at rates less than 1 mm a^{-1}. Conversely, eastern Sicily is subject to small subsidence rates (<-1 mm a^{-1}). Between the coasts of Sicily and North Africa, the island of Pantelleria is subsiding, while Lampedusa and Malta show near null movement. Along the Italian coasts of the Adriatic Sea we find both small subsidence (less than −1 mm a^{-1}) and near-null vertical rates. Particularly along the coasts of the Marche–Abruzzi regions, a few sites show subsidence rates between −2 and −4 mm a^{-1}, while most of the other sites are subject to uplift at rates approaching 1 mm a^{-1}. The northern Adriatic region shows a diffuse pattern of subsidence, with rates larger than −5 mm a^{-1} in the area of Venice. These values decrease toward the NE and are near or uplifting at rates of <1 mm a^{-1} along the coasts of Friuli. Along the eastern Adriatic coast only a few stations are available and these show

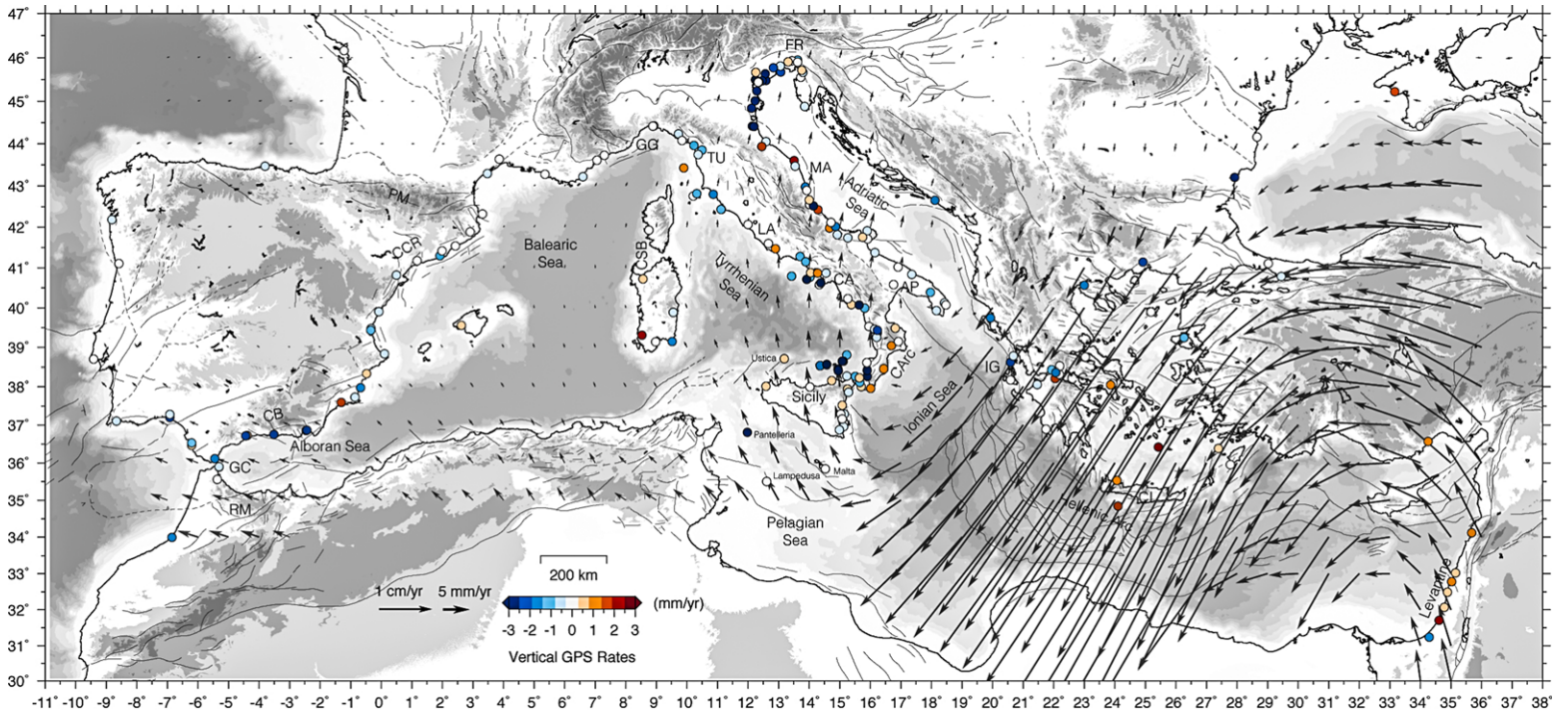

Fig. 8. Plot of the vertical velocities (coloured circles) of cGPS stations located less than 20 km from coastlines, together with a smoothed horizontal velocity field (with respect to a fixed Eurasian frame) interpolated over a regular grid. RM, Riff Mountains; GC, Gulf of Cadiz; CB, Cordillera Betica; CCR, Catalan Coastal Range; PM, Pyrenees Mountains; GG, Gulf of Genoa; TU, Tuscany; LA, Latio–Abruzzi; CA, Campania; CArc, Calabrian arc; AP, Apulia; MA, Marche–Abruzzi; FR, Friuli; IG, Ionian Greece; CI, Crete.

null motion or slow subsidence that increases southward towards the coasts of Ionian Greece where subsidence rates are up to *c.* 2 mm a^{-1}. Along the Hellenic Arc, in the central and eastern Mediterranean, the few available GPS sites show a transition from near-null movements in northern Greece to uplift in Crete, with values decreasing to the east. Finally, along the coasts of the Levant, most of the sites are undergoing small uplift at rates within *c.* 1 mm a^{-1}.

Coasts of the Mediterranean Sea: palaeo-sea-level indicators

In the Mediterranean steep limestone coasts are frequently eroded along near-horizontal horizons forming a so-called 'tidal notch' in cliffs (Pirazzoli *et al.* 1996*a*; Fig. 4b–d) or shore platforms (Sunamura 1992; Kelletat 1997). The notches are considered particularly useful indicators of sea-level change when used in combination with biological indicators such as the presence of the Senegalese fauna in MIS 5e deposits to permit approximate dating (Figs 4e & 9; Lambeck *et al.* 2010*b*). The Senegalese fauna is a faunal assemblage developed during this warm integlacial periods, which includes the gastropod *Persististrombus latus*, Gmelin (formerly named *Strombus bubonius,* Lamarck; Bordoni & Valensise 1998).

The genesis and evolution of tidal notches are still debated. They depend on different factors such as lithology, chemical corrosion (coastal springs and mixing-corrosion), biological erosion by organisms living in the tidal zone, and rate of relative sea-level change owing to either tectonics or climatic changes, and it is often difficult to disentangle the roles of these factors in notch formation (Inman & Nordstrom 1971; De Waele & Furlani 2013). Different types of notches occur in the Mediterranean – structural notches that are controlled by rock strength and abrasion notches that are the result of wave erosion – and can occur at one or several different elevations in the intertidal range or even subtidally (Laborel & Laborel-Deguen 1994). Tidal notches are particularly distinctive on limestone coasts. In many cases they have the deepest point, or vertex, coinciding with mean sea level (Spencer 1988), making them among the most reliable indicators of former sea levels. In more exposed settings, surf benches are formed by wave erosion (Pirazzoli *et al.* 1996*a*), while *trottoirs* are build up by coralline algae (Laborel 1994; Laborel-Deguen 1994) characterized by an accretionary lip. Many studies on the dynamics of notch erosion conducted in the Balearic Islands, Adriatic Sea, and along the coasts of Greece have focused mainly on rates of bio-erosion and karst corrosion. In Sardinia, on the limestone promontories of the Orosei Gulf and Capo Caccia, well-developed

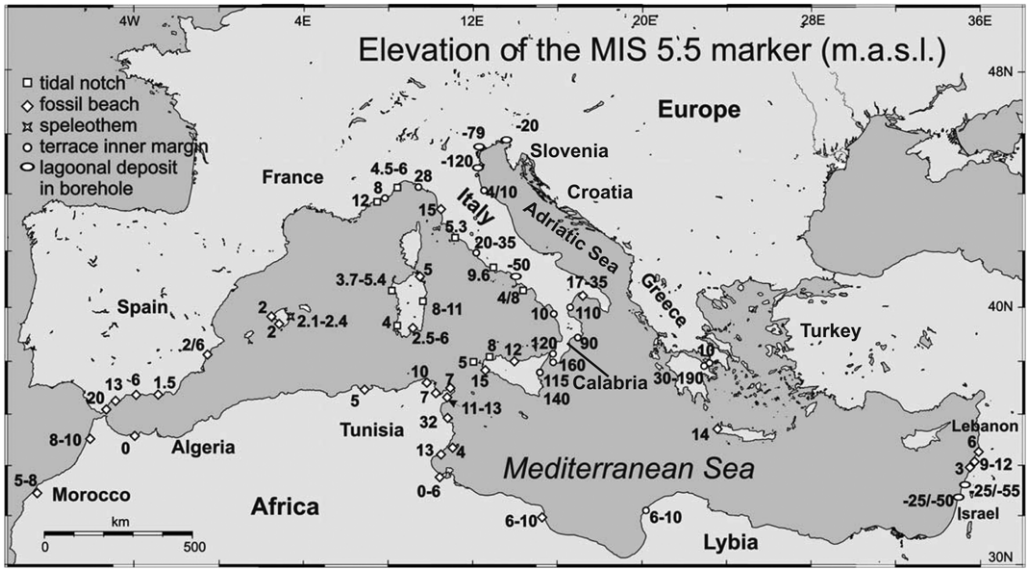

Fig. 9. Elevation of the MIS 5e marker in the Mediterranean region (modified from Ferranti *et al.* 2006). Note the high vertical displacement rates in the Calabrian Arc, which is the region of greatest uplift in the Mediterranean (Ferranti *et al.* 2010). This contrasts with low elevations at sites in North Africa with the one exception of 32 m in Tunisia (Bouaziz *et al.* 2003), or the absence of this horizon in Turkey, suggesting continuous subsiding tectonics.

elevated tidal notches and coastal caves are formed (Fig. 4d, f) by hyperkarst processes and can be up to 1.8 m deep (Antonioli *et al.* 2007).

In addition to the erosional features several other types of palaeo-sea-level indicators are used for determining past sea levels in lowland depositional coastal environments. These include types of siliciclastic deposits, beachrock (Kelletat 2006; Pavlopoulos *et al.* 2009; Vacchi *et al.* 2012*a*, *b*), bioherms built up by corals and coralline algae (Laborel & Laborel-Deguen 1994), and macro- and microfossil distribution (diatoms, testate amoebae, and foraminifera; Belluomini *et al.* 1986). These can provide precise records of local sea-level change, particularly for the period of sea-level rise following the Last Glacial Maximum (Antonioli *et al.* 2004*b*; Lambeck *et al.* 2004*a*). Some of these indicators provide only lower limiting estimates while others provide upper limiting values and the best results are obtained when, from the same location, both types are available, as from the Versilia and Tevere Plains sediment cores (Belluomini *et al.* 1986; Lambeck *et al.* 2010*a*). Good sea-level indicators are organisms that grow fixed to solid substrates near or at sea level. These include Vermetidae, Balanidae, Chthamalidae, Mytilus, Lithophaga, Ostreidae, Serpulidae and coralline algae (Laborel & Laborel-Deguen 1994).

Archaeological data are also valuable for establishing palaeo-sea levels, particularly ancient structures whose functional relationship with sea level is known from written documentation. This is the case of fish tanks and certain harbour structures from the Roman period (Auriemma & Solinas 2009; Fig. 10) and they have provided good evidence of local relative sea level at *c.* 2 ka before present along the coast of Italy (Fig. 10a–e; Lambeck *et al.* 2004*b*), Tunisia (Fig. 10f; Slim *et al.* 2004; Anzidei *et al.* 2011*a*), Libya (Fig. 10g; Anzidei *et al.* 2011*a*), France (Morhange *et al.* 2001), Turkey (Fig. 10h, i), Greece (Fig. 10j; Pavlopoulos 2010; Mourtzas 2012), Israel (Fig. 10k; Anzidei *et al.* 2011*b*) and Spain (Fig. 10l). Such indicators have also provided data on vertical crustal movements in the volcanic areas of Basiluzzo (Tallarico *et al.* 2003) and Baia (Dvorak & Mastrolorenzo 1991), respectively located in the volcanic arc of the Aeolian Islands and the Phlaegrean Fields volcanic complex. The former (Fig. 10e) shows a Roman-age submerged wharf dated at about 2000 years ago that indicates a subsidence of approximately 3.75 m, while the latter subsided more than 5 m since the fourth century AD (Fig. 10d). At the other sites the change over the past 2000 or so years has been much smaller and in Israel, for example, the archaeological evidence indicates that the sea reached a level close to the present one around 2000 years ago, as shown by the fish tank still at its former elevation with respect to sea level (Fig. 10k; Sivan *et al.* 2001, 2004; Toker *et al.* 2011). Recent findings estimated that in Apulia local sea level has risen about 55 cm since the Medieval Warm Period (Pagliarulo *et al.* 2013). Older evidence is given by the Bronze Age harbours (3600 yr B.P.) located in the Levant coast of the Mediterranean (Kraft *et al.* 2003), which indicate about 3 m of submergence (Marriner *et al.* 2006).

The most detailed analysis of the Roman period fish tanks (*piscinae*) is for the relatively stable eastern coasts of the central Tyrrhenian Sea stretching around Rome, where a substantial number of well preserved structures have been examined (Schmiedt 1972). They were generally excavated into solid rock with the flow into and out of the pools controlled by sluice gates and channels and the microtidal range at the time of construction. They are today submerged and no longer functional (Fig. 10b, c) as sea level has locally risen by about 1.35 m in the intervening 2000 years (Lambeck *et al.* 2004*b*).

For all of these observations of past sea levels the question must be asked about the relative roles of land movements, changes in ocean volume and changes in the redistribution of water within evolving ocean basins. This separation can be partly achieved if there are independent markers of tectonic stability. One such is provided by relics of shorelines of the last MIS 5e interglacial period (120–130 ka BP). During this interglacial, the worldwide sea levels in tectonically stable areas were at about 5–7 m above present (Kopp *et al.* 2009; Dutton & Lambeck 2012) with some spatial variability owing to glacio-hydro-isostatic considerations (Lambeck *et al.* 2012). Significant deviation of the MIS 5e marker from the present sea level indicates crustal instability. The MIS 5e event is recorded in many parts of the Mediterranean coast (Ferranti *et al.* 2006, 2010) (Fig. 9). MIS 5e terraces at elevations well above the expected values for tectonically stable areas are found in the Strait of Gibraltar (Zazo *et al.* 1999), in the Gulf of Corinthos Greece (Roberts *et al.* 2009), in northeastern Sicily and southwestern Calabria (Fig. 4g), and Taranto Gulf (Ferranti *et al.* 2006, 2010). In other parts of the Mediterranean basin, such as in Sardinia, Tunisia, Libya and Levant coast, the MIS 5e shorelines are within 7 m of present sea level (Bouaziz *et al.* 2003; Jedoui *et al.* 2003*a*, *b*; Anzidei *et al.* 2011*a*, *b*). In other places they are not visible, such as along the Turkish coasts of the Aegean Sea and the Adriatic coasts (Bruckner 2002; Lambeck *et al.* 2011), either because they have not been preserved through time or, as in the latter region, because of subsidence (Figs 9 & 4h).

Along the coast of northern Africa facing the Mediterranean from Tunisia to Libya, the MIS 5e

levels are generally at 3–7 m above sea level suggesting small, long-term vertical tectonic variaton. One exception occurs near Monastir, Tunisia, where the MIS 5e levels have been identified at up to 32 m in consequence of local tectonic uplift (Anzidei *et al.* 2011*a*; Bouaziz *et al.* 2003). In the Levant region the MIS 5e levels are mostly within 5–7 m of elevation of present sea level (Galili *et al.* 2007), but along the coasts of southwestern Turkey it has not been identified and this is attributed to the tectonic coastal subsidence at about 1.48 mm a^{-1}, associated with the intense seismic activity of the Hellenic Arc (Figs 1 & 5; Anzidei *et al.* 2011*b*). In Italy, the MIS 5e levels occur in the 3–7 m range in many localities, including large sections of the Tyrrhenian coast, corresponding to areas of subdued seismic activity. Elsewhere it departs significantly from this level, both higher, as in parts of Calabria with the highest uplift rates in the Mediterranean decreasing in elevation from about 200 m in the Messina Strait to about 6 m in the southernmost part of Apulia (Figs 4g & 9), and lower, as in the northern Adriatic (Lambeck *et al.* 2004*a*; Ferranti *et al.* 2006). For Greece, France, Spain, Slovenia and Croatia, the MIS 5e data are not homogeneous.

The use of MIS 5e shorelines as reference for tectonic stability assume that the inferred tectonic rates are constant over intervals of 10^5 years but there are localities where clearly this is not valid. One well-known example of variable rates of vertical movement is the Phlaegrean Fields volcanic complex (Lyell 1877). There, the Roman columns of the temple of Serapis show marine borings at elevations up to 7 m above sea level. Radiocarbon dating of *in situ Lithophaga* and other mollusc shells found in the columns, as well as of *in situ* corals and molluscs from nearby cave and cliff sites, indicates that local sea level reached 7 m above present during repeated periods since Roman times: in the fifth century AD, early Middle Ages between 700 and 900 AD, between 1300 and 1500 AD, and finally before 1538, when a volcanic eruption created Monte Nuovo, near Naples (Morhange *et al.* 1999, 2006). Elsewhere, particularly along the Messina Strait, vertical uplift rates inferred from Holocene evidence are up to twice those inferred from the MIS 5e evidence (Lambeck *et al.* 2004*a*). Thus other reference surfaces of tectonic stability are required if the time-dependence of uplift rates is to be examined. For much of the Mediterranean region the glacio-hydro-isostatic contribution to sea level is significant on glacial time scales owing to the loading and gravitational effects of the past ice sheets and the changes in the water loading of the Mediterranean basin (Lambeck & Purcell 2005). These effects are well known (Farrell & Clark 1976; Peltier & Andrews 1976; Nakada & Lambeck 1987; Mitrovica & Milne 2003; Lambeck *et al.* 2003) and models have been globally and regionally tested, including in the Mediterranean (Fig. 11). Thus one approach is to identify sea-level data from areas that are plausibly tectonically stable – as measured by an absence of elevated or submerged older interglacial shorelines or by an absence of instrumental and historical seismicity – and to calibrate the models for earth-rheological parameters that are representative for the region considered. These models then provide the reference surface for estimating uplift and subsidence rates for areas of tectonic interest (Lambeck 1995; Lambeck *et al.* 2004*a*).

Figure 11 provides a quantitative comparison between the model-estimated relative sea level in the Mediterranean at 2 ka BP (Lambeck & Purcell 2005) and the elevations of valid archaeological sea-level markers dated between 1.6 and 2.3 ka BP. This indicates areas of relative vertical tectonic stability that largely follow the patterns established from the seismic and geodetic data, as well as clusters of localities where there has been significant vertical movement over the past 2000 years. In particular, the Roman fish tanks and harbour of Falasarna (Crete) were uplifted about 6.5 m during the 365 AD earthquake (Shaw *et al.* 2008; Fig. 10j) and the Roman city of Baia (Naples) subsided more than 5 m since Roman times (Fig. 10d; Dvorak & Mastrolorenzo 1991). For other areas, such as the northern Adriatic, this comparison shows that subsidence is important, in this case associated with both natural (soil compaction) and anthropogenic (land reclamation, extraction of fluids) interference, and consistent with other geological indicators as well as more recent tide gauge measurements. For

Fig. 10. Archaeological evidence of relative sea-level change in the Mediterranean. (**a**) Roman fish tanks at Briatico (Calabria, Italy). (**b**) Submerged Roman-age fish tank complex of Torre Astura, near Rome (Italy). (**c**) Channel for water exchange within the Roman-age fish tank of Punta della Vipera, near Rome (Italy). (**d**) Submerged mosaics of the Roman city of Baia (Naples, Italy). (**e**) Submerged Roman-age pier built along the volcanic coast of Basiluzzo Island (Aeolian Islands, Italy). (**f**) Submerged Roman-age quarry of Mraissa (Tunisia). (**g**) Lighthouse of the Roman age harbour of Leptis Magna (Libya). (**h**) Submerged bollard at Gemile Island (Turkey). (**i**) Submerged Bizanthyne buildings in the gulf of Fethye (Turkey). (**j**) Uplifted fish tank at Phalasarna (Crete, Greece). (**k**) Roman-age fish tank of Cesarea Marittima (Israel), still at its former position with respect to sea level. (**l**) Roman fish tank at Alicante (Spain). In the latter and (Briatico) the relative sea level has not changed in the last 2 ka owing to a balance of uplift and eustatic–isostatic contributions.

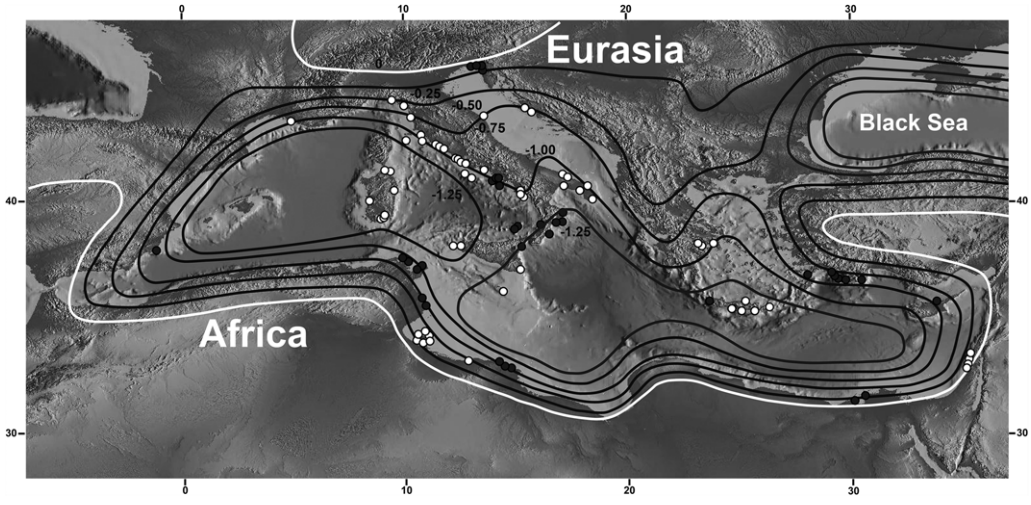

Fig. 11. Estimated relative sea levels and shorelines across the Mediterranean at 2 ka BP (modified from Lambeck & Purcell 2005). The contour interval is 0.25 m. Black contours are negative values and white contour is zero change. Dots are the positions of a set of valid archaeological markers aged between 1.6 and 2.3 ka BP: in white sites those with elevation are in agreement with the sea-level model; in black are those that do not fit the model and are inferred to be vertically displaced by tectonic (or volcanic) activity.

example, near the Po River delta, the subsidence rate is up to 70 mm a^{-1} of which 10–30 mm a^{-1} has been related to fluid (water and hydrocarbons) extraction (Carminati & Martinelli 2002).

These analyses assume that the only contribution to changes in ocean volume during the latter part of the Holocene originates from the residual melting of the large ice sheets and mountain glaciers, with the melting models constrained by global sea-level analyses of geological data (Lambeck *et al.* 2002). It therefore excludes the recent (centennial) changes in ocean volume associated with ocean warming or latest glacier melting recorded in tide-gauge data (Jevrejeva *et al.* 2008; Meyssignac & Cazenave 2012) and high-resolution salt marsh information (Kemp *et al.* 2009). For the last 130 years the instrumental analysis of data collected along the Mediterranean coast indicates a continuous average sea-level rise at a rate of 1.79 ± 0.47 mm a^{-1} (Fig. 12). Such records need to be corrected for both tectonic land movements and for the ongoing earth response to the last deglaciation (Wöppelmann & Marcos 2012). The magnitude of the latter can be approximately derived from Figure 11 and varies from about zero in the easternmost Mediterranean to about $+0.7$ mm yr^{-1} in the central areas such as Sardinia and Crete; some of the spatial variation observed can be attributed to this phenomenon as well as to tectonic contributions. Where tide gauge records co-exist with fish tank data, such as along the Tyrrhenian coast, their comparison, both corrected for the isostatic contributions, indicates that the ocean water volume only started modifying about 100 ± 53 years ago, consistent with it being of recent anthropogenic origin (Lambeck *et al.* 2004*b*).

Geological evidences for past tsunami

Superimposed upon the sea-level signals form eustatic, tectonic and isostatic causes are episodic events that can be attributed to storm surges or tsunami. The latter can be particularly important in the Mediterranean where the active tectonic regime, the diffuse presence of active submarine volcanoes and very steep continental slopes prone to submarine slumps make the coasts prone to the genesis and impact of tsunami. About 10% of reported tsunami in the world occur here, and about 7% of the largest historical earthquakes across the region in the last few thousand years have triggered tsunami (Bryant 2008). The consequences of tsunami within this basin are particularly severe because of the short distances between the tsunamigenic sources and the nearest exposed coasts so that alarms need to be launched with less than an hour before impact. About 300 potential tsunami events have been reported for this area for the last four millennia (Figs 4k & 13; Pirazzoli *et al.* 1999; Soloviev *et al.* 2000; Tinti *et al.* 2007; Shaw *et al.* 2008; Stiros 2010; Mastronuzzi & Sansò 2012; Mastronuzzi *et al.* 2013*a*).

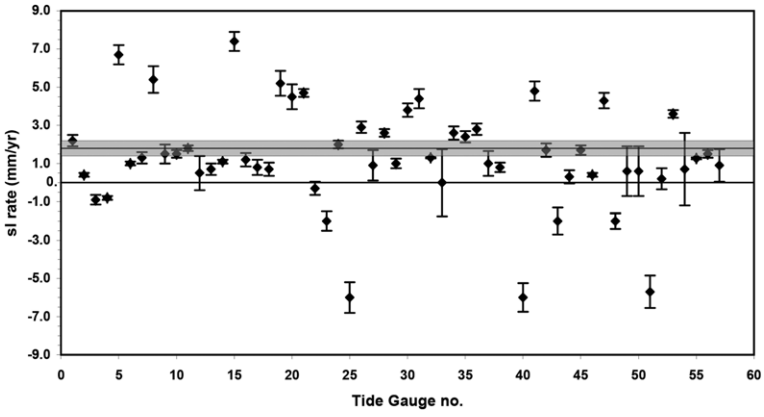

Fig. 12. Plot of the estimated sea-level rates at the 56 analysed tide gauge stations in the Mediterranean and two in the Black Sea. The mean rate estimated in the time span 1884–2011 is 1.79 $\pm$ 0.47 mm a^{-1} (data from www.pol.ac.uk and www.mareografico.it). The horizontal black line is the zero value. The grey band is the mean rate value with uncertainties. No corrections for isostatic or tectonic rates have been applied.

Historical and geological/geomorphologic evidence indicates the episodic impacts of tsunami on rocky and sandy coasts of the Mediterranean, but history, myth and legend are often intertwined with the geological evidence. Examples are the popular legends about the effects of huge waves impacting on coastal human settlements. Procope de Césarée (an author of the sixth century BC), for example, reports the effect of the 'quirks of Porfirione', a sea monster that every 50 years generates waves capable of killing sailors and destroying coastal settlements in the Bosphorus area (Guerra Gotica, VII, 29; Procope de Césarée 1962). Similarly, the myth of Atlantis is frequently correlated with the destruction of the Minoan civilization by the eruption of the Santorini volcano around 1620 BC, associated with a huge tsunami that destroyed ancient settlements in northern Crete (Bruins *et al.* 2008).

Knowledge of tsunami science for the Mediterranean, including the effects caused by distant giant tsunami (Vecchio *et al.* 2012), has improved steadily following the 9 July 1956 event in the Aegean islands (Galanopoulos 1957; Ambraseys 1960; Vacchi *et al.* 2012*a*, *b*), and particularly after the Zemmouri (Algeria) earthquake of 21 May 2003 (Meghraoui *et al*. 2004). Sedimentological and morphological studies performed in subaerial (coastal plains, lagoons and gently sloping rocky coasts) and underwater environments (continental shelves and slope) has led to recognizable tsunami signals (Bridge 2008; Jaffe 2008). These include out-of-place marine sediments interbedded in lagoonal settings, mega-boulders of up to 40 t, with marine bioconcrections, deposited up to tenths of metres inland (Mastronuzzi *et al.* 2006; Scheffers *et al.* 2008; Pignatelli *et al.* 2009; Vella *et al*. 2011; Mastronuzzi & Pignatelli 2012; Shah-Hosseini *et al.* 2013; Fig. 4k), large berms of megaboulders extended up to 13 m above mean sea level) and 200 m inland in southern Italy and Algeria (Nott 2003; Mastronuzzi *et al.* 2007; Shiki *et al.* 2008; Maouche *et al.* 2009), and mega washover fans up to 2 m above mean sea level extending for several square kilometres over the northern part of Lefkada Islands (Greece) and the northern part of Gargano Promontory, Italy (Fig. 4l; Mastronuzzi *et al.* 2013*b*). Evidence also exists for old tsunami striking Greece (Pirazzoli *et al.* 1999; Scheffers & Scheffers 2007; Vött *et al.* 2010), southern Italy (Barbano *et al.* 2010; Mastronuzzi & Sansò 2012), Cyprus (Kelletat & Schellmann 2002; Whelan & Kelletat 2002) and Turkey, Egypt and Algeria. Many of these events are described in historical chronicles, and until recently they were still part of the living memory of the population. The large tsunami that destroyed the cities of Messina and Reggio Calabria (Messina Strait, southern Italy) on 28 December 1908 was caused by a Ms 7.5 earthquake located between Sicily and Calabria (Billi *et al.* 2010), killing several thousand people (Tinti & Armigliato 2003). The run-up was up to 13 m high and the coast underwent a coseismic subsidence up to about 0.7 m, with the area still deforming today (Loperfido 1909; Anzidei *et al.* 1998; Maramai *et al.* 2003; Serpelloni *et al.* 2010).

Specific submarine events that may have triggered tsunami have been identified as marine landslides distributed along the continental scarp of the Mediterranean basin (Ridente *et al.* 2008; Billi *et al.* 2010). Some landslides have been attributed to large inland earthquakes like the 1783 event

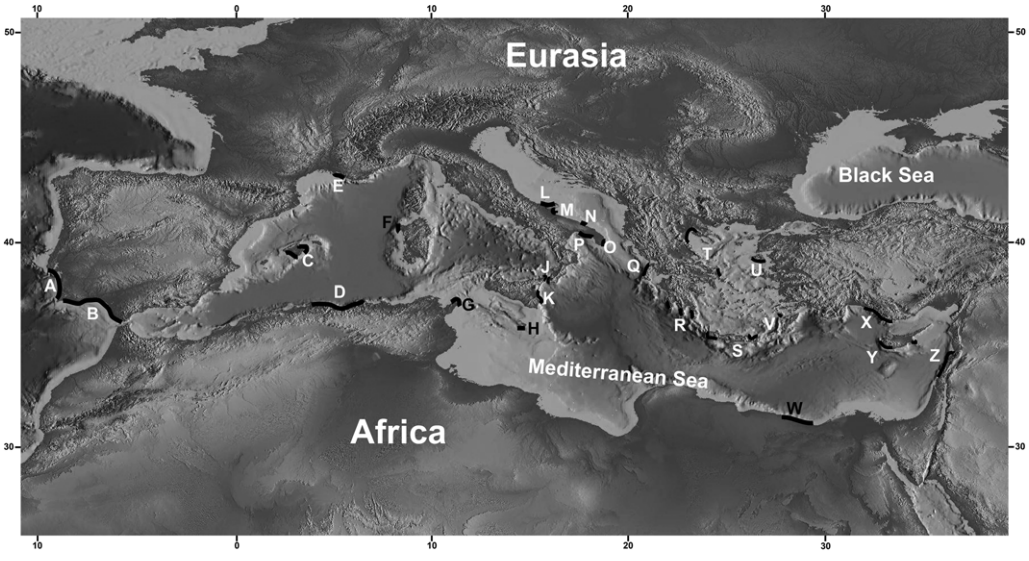

Fig. 13. Map with the location of geomorphologic and sedimentological evidences of the largest tsunami occurred in the Mediterranean between 5660 BP (Crete, Greece) and 1908 (Messina straits, Italy) (Table S1 in the Supplementary Material for details).

that induced the collapse into the sea of a part of Monte Faci near Scilla (Tyrrhenian coast of southern Calabria, location J in Fig. 13; Antonioli *et al.* 2004*b*). The sediments found in the Ionian and Sirte abyssal plains and ascribed to turbidite currents have been correlated to landslides generated by the tsunami that followed the Santorini eruption (Cita & Aloisi 2000). Other landslides have been related to active volcanoes located in the central Mediterranean, such as the destructive 79 AD Vesuvius eruption in Italy (Dvorak & Mastrolorenzo 1991). In the Aeolian Islands, the eruption of Stromboli of 30 December 2002 triggered a slide of the flank of the volcano that generated a tsunami (Maramai *et al.* 2005).

Of the 300 tsunami events in the Mediterranean basin inferred from historical and archaeological data, only 15 have been firmly validated by field evidence and provide a guide for assessing the risk of potential future such events.

Discussion and conclusions

Over the past 125 000 years the Mediterranean basin has experienced great environmental changes owing to tectonic and climate factors that have resulted in major crustal deformation, coastal development and sea-level change on regional and local scales across the region. We have focused on the analysis of coastal zones where these factors combined to produce dramatic changes in the relative elevation of land and sea surfaces as illustrated by the Roman sites of Serapis (Naples, Italy) and at Phalasarna (Crete, Greece). We have reviewed the major sources of evidence for these changes on a time scale ranging from that of modern instrumental records to the longer time scales of historical, archaeological and geological records. In so doing, we have also provided preliminary estimates for the vertical components of these changes. These components have traditionally been more difficult to evaluate than the horizontal motions and displacements using seismic and geodetic evidence representative of recent decades and archaeological and geological evidence for the longer period. Because much of this new information is still preliminary, we have not attempted a detailed comparison of the different methodologies. However a number of common indications occur in the vertical movement patterns around the Mediterranean coast consistently identifying relative stable areas. In these tectonically stable settings significant coastal changes are due to sea-level oscillations driven by the glacial cycles. These type areas are important for calibrating a model for the eustatic/isostatic changes in sea level. This calibrated 'tectonic-free' model then serves as a reference for inferring vertical crustal displacements and for other departures of the actual sea surface from the geoid appropriate for any particular time period. Specifically, it can serve to establish whether an area has been uplifted during the Late Holocene when the Mediterranean eustatic sea level has been estimated not higher

than today, with the possible exception of the far eastern part of the basin. Therefore Holocene coastal deposits located at elevations above (or below) the modern sea level, present clear evidence for local vertical tectonic movements, or that the interpreted deposits are a consequence of tsunami or storm surge activity.

A larger-scale temporal and spatial reconstruction of palaeoshorelines since the LGM can be attempted through this interplay between the observational evidence and geophysical modelling. For the last century it is the seismic and geodetic data that lead to improved interpretations of the land movements, and hence stress and strain conditions, for the tectonically active coastlines. A key problem is whether the short-term rates are representative of the rates on centennial and millennium time scales, particularly as some of the geological analyses have indicated that the average rates for the past 10 000 years can depart significantly from those averaged over 100 000 years (Church *et al.* 2010).

The results obtained in different regions of the Mediterranean of vertical land movements estimated from GPS and seismic data (Figs 5–8) show good agreement between the two datasets as well as with the relative sea-level trends inferred from permanent tidal stations and archaeological observations (Figs 10–12). For example, in the tectonic area of Alicante (Spain), land uplift is evidenced by GPS, levelling data (Giménez *et al.* 2000) and archaeological indicators (this paper), but the estimates of the vertical seismic deformation are still uncertain (Fig. 7). Here, the sea-level trend recorded by the tide gauge station shows a small value of sea-level fall at about 1 mm a^{-1}, consistent with land uplift (Figs 12 & 14). Thus, the balance between the two opposite relative movements is consistent with the current elevation of the Roman fish tank, still at the same position relative to sea level as when it was carved into the rock about 2 ka BP (Fig. 10l). A similar tectonic behaviour occurs along the Tyrrhenian coast of southern Calabria (Italy). Here there is a vertical counterbalance between the tectonic coastal uplift estimated from the seismic (Fig. 7) and relative sea-level change caused by the glacio-hydro-isostasy since the construction of the Roman fish tank at Briatico (Fig. 10a) (Anzidei *et al.* 2013).

Continuous subsidence is inferred from the vertical seismic strain analysis in southwestern Turkey where the tide gauge of Antalya indicates a sea-level rise at 6.8 ± 1.0 mm a^{-1} (Fig. 12) consistent with the submergence of up to -4.5 m of coastal archaeological sites of Byzantine and Roman age (Fig. 10 h, i), stalactites of still unknown age (Fig. 4h; Anzidei *et al.* 2011*b*) and the absence of MIS 5e shoreline markers. Estimates of tectonic subsidence rates range up to to -12 mm a^{-1} (Fig. 7). The tectonically stable coasts of Latium in the Tyrrhenian Sea, Italy (Lambeck *et al.* 2004*b*; Lambeck *et al.* 2010*a*), in Israel (Anzidei *et al.* 2011*b*) and part of northern Africa (Libya and Tunisia; Anzidei *et al.* 2011*a*) are representative of the glacio-hydro-isostatic signal acting in the Mediterranean basin, particularly in its central part. In Israel the different contributions to the glacio-hydro-isostatic effect cancel out (Figs 11 & 14) and the vertical seismic deformation is null along the coast (Fig. 7), in good agreement with the observed GPS uplift (Fig. 8; <1 mm a^{-1}). This combined evidence is consistent with the submergence of the Roman fish tanks of only a few centimetres (Fig. 10k). In North Africa, where instrumental data are lacking, a small misfit between archaeological observations and sea-level predictions is observed, probably owing to still unrecognized local disturbances or uncertainties of the modelling and interpretation of the observations (Figs 10f, g & 11; Anzidei *et al.* 2011*a*). Along the seismically and geodetically established tectonically stable coast of Latium near Rome, the elevation of the Roman fish tanks is consistent with the sea-level predictions and these coastal sites are submerged by about -1.35 m on average (Figs 10b, c & 11) as a result of the glacio-hydro-isostatic factor. Comparison with nearby tide gauge records led to the conclusion that, if the recorded rates (corrected for the isostatic effects) are extrapolated back in time, then the Roman epoch levels have been reached within the last 100 ± 53 years (Lambeck *et al.* 2004*b*), reinforcing the hypothesis of a recent acceleration in sea-level variations and supporting the interpretations of the anthropogenic contribution to the observed global change (IPCC 2007; Rahmstorf *et al.* 2007; Lambeck *et al.* 2010*b*; Gehrels & Woodworth 2013). Figure 14 shows the estimated relative sea levels in the Mediterranean at 2 ka BP (Lambeck & Purcell 2005) and the trends of land uplift, subsidence or stability (indicated with $+$, $-$ and 0 respectively) that influence the local sea-level rise. Submerging coasts undergoing or prone to flooding hazard are shown in red. Although our current models are inadequate for long-term extrapolation owing to an incomplete instrumental record, they establish areas where the signs of the tectonic changes are such as to either compensate for or intensify the recent climate change signal, and to identify areas at above normal flooding risk owing to any future changes in ocean volume. This information should be valuable in planning coastal land use to minimize the risk of damaging floods during recurring large seas storms. The Mediterranean populations are, however, unprepared to deal with the effects of very rare, but larger extreme events like tsunami that are known to have occurred in

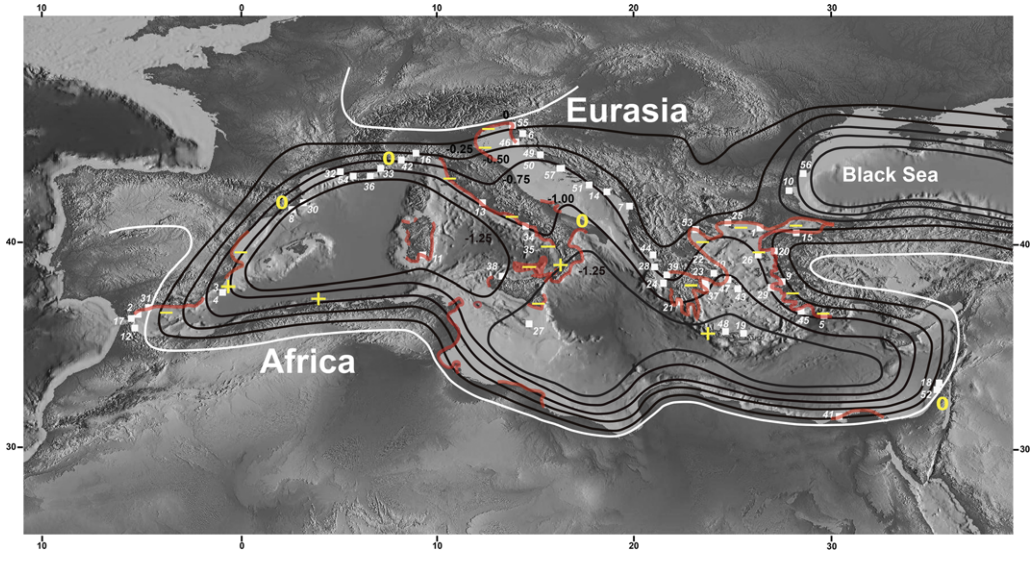

Fig. 14. Estimated relative sea levels and shorelines across the Mediterranean at 2 ka BP (modified from Lambeck & Purcell 2005). The contour interval is 0.25 m. Black contours are negative values, white contour is zero change. The +, − and 0 indicate locations of land uplift, subsidence or stability, respectively. Submerging coasts undergoing or expected to flood owing to sea-level rise, storm surge and tsunami are shown in red, as inferred from the seismic, geodetic, geological and archaeological evidence. White squares are the positions of a set of tidal stations from which the current sea-level trend shown in Figure 13 has been estimated (station numbers correspond to the tide gauge identification of Figure 13: 1, Alexandropoulis; 2, Algeciras; 3, Alicante I; 4, Alicante II; 5, Antalya; 6, Bakar; 7, Bar; 8, Barcelona; 9, Bodrum; 10, Bourgas; 11, Cagliari; 12, Ceuta; 13, Civitavecchia; 14, Dubrovnik; 15, Erdek; 16, Genova; 17, Gibraltar; 18, Hadera; 19, Iraklion; 20, Izmir; 21, Kalamai; 22, Khalkis North; 23, Khalkis South; 24, Katakolon; 25, Kavalla; 26, Khios; 27, La Valletta; 28, Lefkas; 29, Leros; 30, L'Estartit; 31, Malaga II; 32, Marseille; 33, Monaco; 34, Napoli Arsenale; 35, Napoli Mandraccio; 36, Nice; 37, North Salaminos; 38, Palermo; 39, Patrai; 40, Piraeius; 41, Port Said; 42, Porto Maurizio; 43, Posidhonia; 44, preveza; 45, Rodos; 46, Rovinji; 47, Siros; 48, Soudhas; 49, Split RT; 50, Split GL; 51, Sucuraji; 52, Tel Aviv; 53, Thessaloniki; 54, Toulon; 55, Trieste; 56, Varna; 57, Zadar.

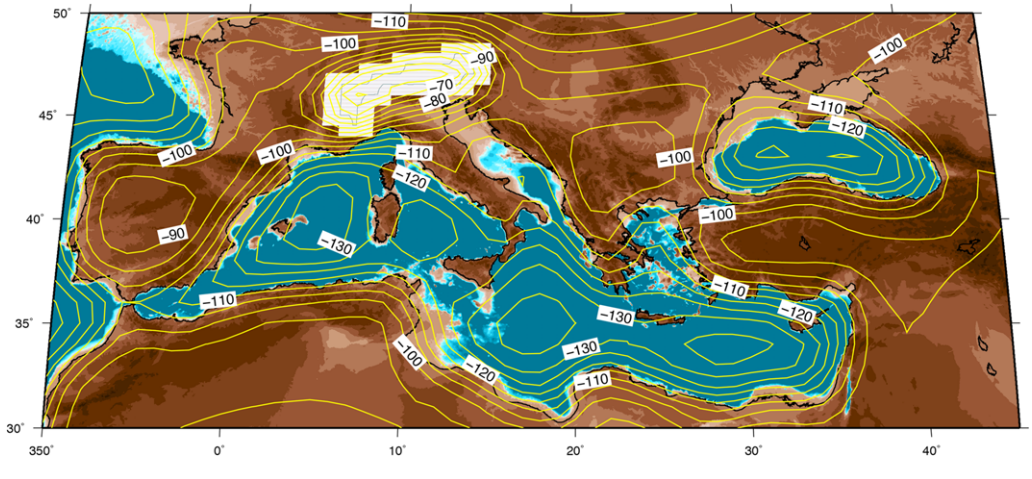

Fig. 15. Palaeogeographic reconstruction of the Mediterranean basin for the time of the Last Glacial Maximum at 20 000 years BP, predicted using the eustatic-isostatic ice model 19_10_16_10 and Earth model ma2A_20 (after Lambeck & Purcell 2005). Contours show the sea-level change with respect to present sea level (contour interval is 5 m). Corresponding values for the Alps are indicated by the white zone.

preferred areas but whose recurrence and intensity cannot be predicted.

Once the uplift/subsidence and sea-level histories are established, it becomes possible to model the coastline geometries through time. Until now this has only been attempted for parts of the Mediterranean for the past 20 000 years, on the assumption that the dominant contribution on this time scale is from the eustatic and glacio-hydro-isostatic components (Lambeck 1996; Lambeck *et al.* 2004*a*). A basin-wide reconstruction is shown in Figure 15 for the time of the LGM that illustrates the large spatial variation in sea-level change across the region, from less than 100 m in the northern Adriatic Sea to more than 130 m in the central part of the basin. Extensive exposed shelves at lowstand include the northern Adriatic, the Gulf of Gabez between Tunisia and Libya, the Gulf of Valencia and the Gulf du Lyon in the NW and parts of the Aegean including the exposed Cycladean Plateau, and the southern extensions of Sicily to Malta and towards Pantelleria. The rise in sea level across the Mediterranean following the LGM is generally sufficiently well known to map the evolution of the flooding of these areas (Rovere *et al.* 2012) and to begin to address archaeological questions, for example, to establish (a) the timing of the submergence of the entry to Cosquer Cave near Marseilles (Clottes & Courtin 1994) and hence a minimum age for human occupation (Lambeck & Bard 2000); (b) whether sophisticated sailing and navigational skills were required for the earliest transport of obsidian from Melos in the Cycladean island group to the Franchthi Cave in Argolis the end of the Palaeolithic period (*c.* 10 900 BS; Renfrew & Aspinall 1987; Lambeck 1996); and (c) the timing of the isolation of Sicily from mainland Italy and tidal conditions at the time of the early flooding of the Messina Strait (Antonioli *et al.* 2014).

This work has been funded by the Flagship Project RITMARE – The Italian Research for the Sea – coordinated by the Italian National Research Council and by the Italian Ministry of Education, University and Research within the National Research Program 2011–2013 and by the Progetto di Ricerca COFIN MIUR 2010–2011 'Response of morphoclimatic system dynamics to global changes and related geomorphologic hazard'. The paper is an Italian contribution to the project IGCP 588 – International Geological Correlation Programme 'Preparing for coastal change. A detailed response process framework for coastal change at different times' by UNESCO–IUGS (project leaders Dr A. D. Switzer, Earth Observatory of Singapore, Nanyang Technological University, Dr C. Sloss, School of Natural Resources Sciences, Queensland University of Technology, Australia, Dr B. Horton, Department of Earth and Environmental Sciences, University of Pennsylvania, Dr Y. Zong, Department of Earth Sciences, University of Hong Kong, China). This study has been partially carried out under the umbrella of the MEDFLOOD project, funded by INQUA (project 1202P). We are particularly thankful to I. P. Martini and to the anonymous reviewers for their fruitful suggestions that contributed to improve this manuscript.

References

Altamimi, Z., Collilieux, X. & Métivier, L. 2011. ITRF2008: an improved solution of the international terrestrial reference frame. *Journal of Geodesy*, **85**, 457–473.

Ambraseys, N. N. 1960. The seismic sea wave of July 9, 1956, in the Greek Archipelago. *Journal of Geophysical Research*, **65**, 1257–1265.

Antonioli, F., Bard, E., Potter, E. K., Silenzi, S. & Improta, S. 2004*a*. 215-ka History of sea-level oscillations from marine and continental layers in Argentarola Cave speleothems. *Global and Planetary Change*, **43**, 57–78.

Antonioli, F., Dai Pra, G., Segre, A. G. & Sylos Labini, S. 2004*b*. New data on Late Holocene uplift rates in the Messina Strait area, Italy. *Quaternaria Nova*, **8**, 45–67.

Antonioli, F., Anzidei, M. *et al.* 2007. Sea level change during Holocene from Sardinia and northeastern Adriatic from archaeological and geomorphological data. *Quaternary Science Review*, **26**, 2463–2486.

Antonioli, F., Lo Presti, V. *et al.* 2014. Timing of the emergence of the Europe–Sicily bridge (40–17 ka cal BP) and its implications for the spread of modern humans. *In*: Harff, J., Bailey, G. & Lüth, F. (eds) *Geology and Archaeology: Submerged Landscapes of the Continental Shelf*. The Geological Society, London, Special Publications, **411**, http://dx.doi.org/10.1144/SP411.1

Anzidei, M., Baldi, P., Bonini, C., Casula, G., Gandolfi, S. & Riguzzi, F. 1998. Geodetic surveys across the Messina Straits (southern Italy) seismogenetic area. *Journal of Geodynamics*, **25**, 85–97.

Anzidei, M., Antonioli, F., Lambeck, K., Benini, A. & Soussi, M. 2011*a*. New insights on the relative sea level change during Holocene along the coasts of Tunisia and western Libya from archaeological and geomorphological markers. *Quaternary International*, **232**, 5–12.

Anzidei, M., Antonioli, F., Benini, A., Lambeck, K., Sivan, D., Serpelloni, E. & Stocchi, P. 2011*b*. Sea level change and vertical land movements since the last two millennia along the coasts of southwestern Turkey and Israel. *Quaternary International*, **232**, 13–20.

Anzidei, M., Antonioli, F., Benini, A., Gervasi, A. & Guerra, I. 2013. Evidence of vertical tectonic uplift at Briatico (Calabria, Italy) inferred from Roman age maritime archaeological indicators. *Quaternary International*, **288**, 158–167.

Auriemma, R. & Solinas, E. 2009. Archaeological remains as sea level change markers: a review. *Quaternary International*, **206**, 1–13.

Barbano, M. S., Pirrotta, C. & Gerardi, F. 2010. Large boulders along the south-eastern Ionian coast of Sicily: storm or tsunami deposits? *Marine Geology*, **275**, 140–154.

BELLUOMINI, G., IUZZOLINI, P., MANFRA, L., MORTARI, R. & ZALAFFI, M. 1986. Evoluzione recente del delta del Tevere. *Geologica Romana*, **25**, 213–234.

BENNET, R. A., SERPELLONI, E. *ET AL.* 2012. Syn-convergent extension observed using the RETREAT GPS network, northern Apennines, Italy. *Journal of Geophysical Research, Solid Earth*, **117**, B4.

BILLI, A., MINELLI, L., ORECCHIO, B. & PRESTI, D. 2010. Constraints to the cause of three historical tsunami (1908, 1783, and 1693) in the Messina straits region, Sicily, southern Italy. *Seismological Research Letters*, **81**, 6.

BORDONI, P. & VALENSISE, G. 1998. Deformation of the 125 ka marine terrace in Italy: tectonic implications. *In*: STEWART, I. S. & VITA-FINZI, C. (eds) *Coastal Tectonics*. Geological Society, London, Special Publications, **146**, 71–110.

BOUAZIZ, S., JEDOUI, Y., BARRIER, E. & ANGELIER, J. 2003. Neotectonique affectant les dépots marins tyrrhéniens du littoral sud-est tunisien: implications pour les variations du niveau marin. *Comptes Rendus Geoscience*, **335**, 247–254.

BRAUNMILLER, J., KRADOLFER, U. & GIARDINI, D. 2002. Regional moment tensor determination in the European Mediterranean area – initial results. *Tectonophysics*, **356**, 5–22.

BRIDGE, J. S. 2008. Discussion of articles in 'Sedimentary features of tsunami deposits'. *Sedimentary Geology*, **211**, 94.

BRUCKNER, H. 2002. Holocene landscape evolution of Buyuk Menderes. *Zeitschrift für Geomorphologie*, **127**, 47–65.

BRUINS, H. J., MACGILLIVRAY, J. A. *ET AL.* 2008. Geoarchaeological tsunami deposits at Palaikastro (Crete) and the Late Minoan IA eruption of Santorini. *Journal of Archaeological Science*, **35**, 191–212.

BRYANT, E. A. 2008. *Tsunami. The Underrated Hazard*. Springer, New York, **325**.

CARMINATI, E. & MARTINELLI, G. 2002. Subsidence rates in the Po Plain, northern Italy: the relative impact of natural and anthropogenic causation. *Engineering Geology*, **66**, 241–255.

CAROBENE, L. & DAI PRA, G. 2003. Middle and Upper Pleistocene sea-level highstands along the Tyrrehenian coast of Basilicata (southern Italy). *Il Quaternario*, **4**, 173–202.

CHURCH, J. A., WOODWORTH, P. L., AARUP, T. & WILSON, W. S. 2010. *Understanding Sea-level Rise and Variability*. Wiley-Blackwell, Oxford.

CITA, M. B. & ALOISI, G. 2000. Deep-sea tsunami deposits triggered by the explosion of Santorini (3500y BP), eastern Mediterranean. *Sedimentary Geology*, **135**, 181–203.

CLOTTES, J. & COURTIN, J. 1994. *La Grotte Cosquer*. Editions du Seuil, Paris.

DE WAELE, J. & FURLANI, S. 2013. Seawater and biokarst effects on coastal limestones. *In*: SHRODER, J. & FRUMKIN, A. (eds) *Treatise on Geomorphology*. Academic Press, San Diego, CA, **9**, 342–351.

DEWEY, J. F., PITMAN, W. C., RYAN, W. B. F. & BONNIN, J. 1973. Plate tectonics and the evolution of the Alpine system. *Geological Society America Bulletin*, **84**, 3137–3180.

DONG, D., FANG, P., BOCK, Y., CHENG, M. & MIYAZAKI, S. 2002. Anatomy of apparent seasonal variations from GPS-derived site position time series. *Journal of Geophysical Research*, **107**, http://dx.doi.org/10.1029/2001JB000573

DONG, D., FANG, P., BOCK, Y., WEBB, F., PRAWIRODIRDJO, L., KEDAR, S. & JAMASON, P. 2006. Spatiotemporal filtering using principal component analysis and Karhunen–Loeve expansion approaches for regional GPS network analysis. *Journal of Geophysical Research*, **111**, B03405, http://dx.doi.org/10.1029/2005JB003806

DORALE, J. P., ONAC, B. *ET AL.* 2010. Sea-level highstand 81,000 years ago in Mallorca. *Science*, **327**, 860–863.

DUGGEN, S., HOERNLE, K., VAN DEN BOGAARD, P., RUPKE, L. & PHILIPS MORGAN, J. C. 2003. Deep roots for the Messinian salinity crisis. *Nature*, **422**, 602–606.

DUMAS, B., GUEREMY, P., LHENAFF, R. & RAFFY, J. 1993. Rapid uplift, stepped marine terraces and raised shorelines on the Calabrian coast of the Messina Straits, Italy. *Earth Surface Processes and Landforms*, **18**, 241–256.

DUTTON, A. & LAMBECK, K. 2012. Ice volume and sea level during the last interglacial. *Science*, **337**, 216–219.

DVORAK, J. J. & MASTROLORENZO, G. 1991. The mechanisms of recent vertical crustal movements in Campi Flegrei caldera, Southern Italy. *Special Paper of the Geological Society of America*, **263**, 1–47.

EKSTRÖM, G., DZIEWONSKI, A. M., MATERNOSVSKAYA, N. N. & NETTLES, M. 2005. Global seismicity of 2003: Centroid-moment tensor solutions for 1087 earthquakes. *Physics of the Earth and Planetary Interior*, **148**, 327–351.

FARRELL, W. E. & CLARK, J. A. 1976. On postglacial sea-level. *Geophysical Journal*, **46**, 79–116.

FERRANTI, L., ANTONIOLI, F. *ET AL.* 2006. Markers of the last interglacial sea-level high stand along the coast of Italy: tectonic implications. *Quaternary International*, **145**, 30–54.

FERRANTI, L., ANTONIOLI, F., ANZIDEI, M., MONACO, C. & STOCCHI, P. 2010. The timescale and spatial extent of vertical tectonic motions in Italy: insights from relative sealevel changes studies. *Journal of the Virtual Explorer*, **36**, 30, http://virtualexplorer.com.au/

FLEMMING, N. & WEBB, C. O. 1986. Tectonic and eustatic coastal changes during the last 10,000 years derived from archaeological data. *Zeitschrift fur Geomorphologie. N.F.*, **62**, 1–29.

FROHLICH, C. 1992. Triangle diagrams: ternary graphs to display similarity and diversity of earthquake focal mechanisms. *Physics of the Earth and Planetary Interior*, **75**, 193–198.

FURLANI, S., ANTONIOLI, F. *ET AL.* 2013. Holocene sea level change in Malta. *Quaternary International*, **XX**, 1–12, http://dx.doi.org/10.1016/j.quaint.2012.02.038

GALANOPOULOS, A. G. 1957. The seismic sea wave of July 9, 1956. *Praktika Akadimias, Athenon*, **32**, 90–101.

GALILI, E., ZVIELY, D., RONEN, A. & MIENIS, H. K. 2007. Beach deposits of MIS 5e high sea stand as indicators

for tectonic stability of the Carmel coastal plain, Israel. *Quaternary Science Reviews*, **26**, 2544–2557.

Garcia-Castellanos, D., Estrada, F., Jimenez-Munt, I., Gorini, C., Fernandez, M., Verges, J. & de Vicente, R. 2009. Catastrophic flood of the Mediterranean after the Messinian salinity crisis. *Nature*, **462**, 778–781.

Gehrels, W. R. & Woodworth, P. L. 2013. When did modern rates of sea-level rise start? *Global and Planetary Change*, **100**, 263–277, http://dx.doi.org/10.1016/j.gloplacha.2012.10.020

Giménez, J., Suriñach, E. & Goula, X. 2000. Quantification of vertical movements in the eastern Betics (Spain) by comparing levelling data. *Tectonophysics*, **317**, 237–258.

Giménez, J., Borque, M. J., Gil, A., Alfaro, P., Estévez, A. & Surinach, E. 2009. Comparison of long-term and short-term uplift rates along an active blind reverse fault zone (Bajo Segura, Se Spain). *Studia Geophysica et Geodaetica*, **53**, 81–98.

Goy, J. L. & Zazo, C. 1988. Sequences of Quaternary marine levels in Elche Basin (eastern Betic Cordillera, Spain). *Palaegeography, Palaeoclimatology, Palaeoecology*, **68**, 301–310.

Guidoboni, E. 1994.*Catalogue of Ancient Earthquakes in the Mediterranean Area Up to the 10th Century*. Istituto Nazionale di Geofisica, Rome.

Guidoboni, E. & Comastri, A. 2007. *Catalogue of Earthquakes and Tsunami in the Mediterranean Area from the 11th to the 15th Century*. Istituto Nazionale di Geofisica e Vulcanologia, Bologna.

Herring, T., King, R. W. & McClusky, S. 2010. *GAMIT Reference Manual, Release 10.4*. Massachussetts Institute of Technology, Cambridge, MA.

Hollenstein, Ch., Kahle, H. G., Geiger, A., Jenny, S., Goes, S. & Giardini, D. 2003. New GPS constraints on the Africa-Eurasia plate boundary zone in southern Italy. *Geophysical Research Letters*, **30**, 18, 1935, http://dx.doi.org/10.1029/2003GL017554

Hsu, K. J., Ryan, W. B. F. & Cita, M. B. 1973. Late Miocene dessication of the Mediterranean. *Nature*, **242**, 240–244.

Inman, D. L. & Nordstrom, C. E. 1971. On the tectonic and morphologic classification of coasts. *Journal of Geology*, **79**, 1–21.

IPCC 2007. Summary for policymakers. Contribution of Working Group I to the Fourth Assessment Report of the Intergovernmental Panel on Climate Change. *In*: Solomon, S., Qin, D., Manning, M., Chen, Z., Marquis, M., Averyt, K. B., Tignor, M., Miller, H. L. (eds) *Climate Change 2007: The Physical Science Basis*. Cambridge University Press, Cambridge.

ISC 2001. On-line Bulletin. International Seismological Center, Thatcham, http://www.isc.ac.uk/Bull (accessed 28 March 2013).

Jackson, J. & McKenzie, D. 1988. The relationship between plate motions and seismic moment tensors, and the rates of active deformation in the Mediterranean and Middle-East. *Geophysical Journal International*, **93**, 45–73.

Jaffe, B. 2008. The role of deposits in tsunami risk assessment. *In*: Wallendorf, L., Ewing, L., Jones, C. & Jaffe, B. (eds) *Proceedings of the conference 'Solutions to Coastal Disasters 2008: Tsunamis'*, *Turtle Bay, Oahu, Hawaii, United States, April 13–16, 2008*. American Society of Civil Engineers, Reston, VA, 256–267, http://dx.doi.org/10.1061/40978(313)24

Jedoui, Y., Reyss, J. L., Jallel, N., Montacer, M., Ismail, H. B. & Davaud, E. 2003*a*. U-series evidence for two high Last Interglacial sea levels in southeastern Tunisia. *Quaternary Science Reviews*, **22**, 343–351.

Jedoui, Y., Kallel, N., Fontugne, M., Ben Ismail, H., M'Rabet, A. & Montacer, M. 2003*b*. A high relative sea-level stand in the middle Holocene of southeastern Tunisia. *Marine Geology*, **147**, 123–130.

Jevrejeva, S., Moore, J. C., Grinsted, A. & Woodworth, P. L. 2008. Recent global sea level acceleration started over 200 years ago? *Geophysical Research Letters*, **35**, L08715.

Kelletat, D. 1997. Mediterranean coastal biogeomorphology: processes, forms, and sea-level indicators. *In*: Briand, F. & Maldonado, A. (eds) *Transformations and Evolution of the Mediterranean Coastline*. Commission Internationale pour l'Exploration Scientifique de la mer Méditerranée Science Series **3**, *Bulletin de L'Institut océanographique, Monaco* (numéro spécial), **18**, 209–226.

Kelletat, D. 2006. Beachrock as sea level indicator? Remarks from a geomorphological point of view. *Journal of Coastal Research*, **22**, 1558–1564.

Kelletat, D. & Schellmann, G. 2002. Tsunamis on Cyprus: field evidences and ^{14}C dating results. *Zeitschrift fur Geomorphologie, N.F.*, **46**, 19–34.

Kemp, A. C., Horton, B. P. *et al.* 2009. Timing and magnitude of recent accelerated sea-level rise (North Carolina, United States). *Geology*, **37**, 1035–1038.

Keraudren, B. & Sorel, D. 1987. The terraces of Corinth (Greece) – a detailed record of eustatic sea-level variations during the last 500,000 years. *Marine Geology*, **77**, 99–107.

Kiratzi, A. A. & Papazachos, C. B. 1995. Active crustal deformation from the Azores Triple junction to the Middle East. *Tectonophysics*, **243**, 1–24.

Kopp, R. E., Simons, F. J., Mitrovica, J. X., Maloof, A. C. & Oppenheimer, M. 2009. Probabilistic assessment of sea level during the last interglacial stage. *Nature*, **462**, 863–868.

Kostrov, V. V. 1974. Seismic moment and energy of earthquakes and seismic flow of rocks. *Physics of the Solid Earth*, **1**, 13–21.

Kraft, J. C., Rapp, G., Kayan, I. & Luce, J. V. 2003. Harbor areas at ancient Troy: sedimentology and geomorphology complement Homer's Iliad. *Geology*, **31**, 163–166.

Laborel, J. & Laborel-Deguen, F. 1994. Biological indicators of relative sea-level variation and of co-seismic displacements in the Mediterranean area. *Journal of Coastal Research*, **10**, 395–415.

Lambeck, K. 1995. Late Pleistocene and Holocene sea-level change in Greece and south-western Turkey: a separation of eustatic, isostatic and tectonic contributions. *Geophysical Journal International*, **122**, 1022–1044.

Lambeck, K. 1996. Sea-level change and shore-line evolution in Aegean Greece since Upper Palaeolithic time. *Antiquity*, **70**, 588–611.

LAMBECK, K. & BARD, E. 2000. Sea-level change along the French Mediterranean coast since the time of the Last Glacial Maximum. *Earth Planetary Science Letters*, **175**, 203–222.

LAMBECK, K. & PURCELL, A. 2005. Sea-level change in the Mediterranean since the LGM: model predictions for tectonically stable areas. *Quaternary Science Reviews*, **24**, 1969–1988.

LAMBECK, K., YOKOYAMA, Y. & PURCELL, T. 2002. Into and out of the last glacial maximum: sea-level changes during oxygen isotope stages 3 and 2. *Quaternary Science Reviews*, **21**, 343–360.

LAMBECK, K., PURCELL, A., JOHNSTON, P., NAKADA, M. & YOKOYAMA, Y. 2003. Water-load definition in the glacio-hydro-isostatic sea-level equation. *Quaternary Science Reviews*, **22**, 309–318.

LAMBECK, K., ANTONIOLI, F., PURCELL, A. & SILENZI, S. 2004*a*. Sea-level change along the Italian coast for the past 10,000 yrs. *Quaternary Science Reviews*, **23**, 1567–1598.

LAMBECK, K., ANZIDEI, M., ANTONIOLI, F., BENINI, A. & ESPOSITO, A. 2004*b*. Sea level in Roman times in the Central Mediterranean and implications for recent change. *Earth and Planetary Science Letters*, **224**, 563–575.

LAMBECK, K., ANTONIOLI, F. & ANZIDEI, M. 2010*a*. Sea level change along the Tyrrhenian coast from early Holocene to the present. *Accademia Nazionale dei Lincei, IX Giornata mondiale dell'acqua, Il bacino del Tevere*, Roma, Atti dei convegni Lincei, **254**, 11–26.

LAMBECK, K., WOODROFFE, C. D., ANTONIOLI, F., ANZIDEI, M., GEHRELS, W. R., LABOREL, J. & WRIGHT, A. J. 2010*b*. Paleoenvironmental records, geophysical modeling, and reconstruction of sea-level trends and variability on centennial and longer timescales. *In*: WOODWORTH, P. L., AARUP, T. & WILSON, W. S. (eds) *Understanding Sea Level Rise and Variability*. Blackwell, Oxford, 61–121.

LAMBECK, K., ANTONIOLI, F., ANZIDEI, M., FERRANTI, L., LEONI, G., SCICCHITANO, G. & SILENZI, S. 2011. Sea level change along the Italian coast during the Holocene and projections for the future. *Quaternary International*, **232**, 250–257.

LAMBECK, K., PURCELL, A. & DUTTON, A. 2012. The anatomy of interglacial sea levels: the relationship between sea levels and ice volumes during the Last Interglacial. *Earth Planetary Science Letters*, **315–316**, 4–11.

LE PICHON, X., BERGERAT, F. & ROULET, M. J. 1988. *Plate Kinematics and Tectonics Leading to the Alpine Belt Formation: a New Analysis*. Geological Society of America, Boulder, CO, Special Papers, **218**, 111–131.

LOPERFIDO, A. 1909. Livellazione geometrica di precisione eseguita dall'IGM sulla costa orientale della Sicilia, da Messina a Catania, a Gesso ed a Faro Peloro e sulla costa occidentale della Calabria da Gioia Tauro a Melito di Porto Salvo. *Reale Accademia Nazionale dei Lincei*, **35**, 131–155.

LYELL, C. 1877. *Principles of Geology*, 12th edn. Appleton, New York.

MAOUCHE, S., MORHANGE, Ch. & MEGHRAOUI, M. 2009. Large boulder accumulation on the Algerian coast evidence tsunami events in the western Mediterranean. *Marine Geology*, **262**, 96–104.

MARAMAI, A., GRAZIANI, L. & TINTI, S. 2003. Updating and revision of the European Tsunami Catalogue. *In*: YALCINER, A. C., PELINOVSKY, E., OKAL, E. & SYNOLAKIS, C. (eds) *NATO Sciences Series: Submarine Landslides and Tsunamis*. Kluwer Academic, Dordrecht, 25–32.

MARAMAI, A., GRAZIANI, L. & TINTI, S. 2005. Tsunamis in the Aeolian Islands (southern Italy): a review. *Marine Geology*, **215**, 11–21.

MARRINER, N., MORHANGE, C., DOUMET-SERHAL, C. & CARBONEL, P. 2006. Geoscience rediscovers Phoenicia's buried harbors. *Geology*, **34**, 1–4.

MASTRONUZZI, G. & PIGNATELLI, C. 2012. The boulders berm of Punta Saguerra (Taranto, Italy): a morphological imprint of 4th April, 1836 Rossano Calabro tsunami? *Earth Planets Space*, **64**, 829–842.

MASTRONUZZI, G. & SANSÒ, P. 2002. Holocene uplift rates and historical rapid sea-level changes at the Gargano promontory, Italy. *Journal of Quaternary Science*, **17**, 593–606.

MASTRONUZZI, G. & SANSÒ, P. 2012. The role of large earthquakes and tsunami in the Late Holocene evolution of Fortore River coastal plain (Apulia, Italy): a synthesis. *Geomorphology*, **138**, 89–99.

MASTRONUZZI, G., PIGNATELLI, C. & SANSÒ, P. 2006. Boulder fields: a valuable morphological indicator of paleotsunami in the Mediterranean Sea. *Zeitschrift für Geomorphologie, N.F. Suppl.-Bd.*, **146**, 173–194.

MASTRONUZZI, G., PIGNATELLI, C., SANSÒ, P. & SELLERI, G. 2007. Boulder accumulations produced by the 20th February 1743 tsunami along the coast of southeastern Salento (Apulia region, Italy). *Marine Geology*, **242**, 191–205.

MASTRONUZZI, G., BRÜCKNER, H., DE MARTINI, P. M. & REGNAULD, H. 2013*a*. Tsunami: from the open sea to the coastal zone and beyond. *In*: MAMBRETTI, S. (ed.) *Tsunami: Primary Causes to Mitigation*. WIT Press, Southampton, **168**, 1–36.

MASTRONUZZI, G., CALCAGNILE, L., PIGNATELLI, C., QUARTA, G., STAMATOPOULOS, L. & VENISTI, N. 2013*b*. Late Holocene tsunamogenic coseismic uplift in Kerkyra Island, Greece. *Quaternary International*, **332**, 48–60, http://dx.doi.org/10.1016/j.quaint.2013.10.042

MEGHRAOUI, M., MAOUCHE, S. *ET AL*. 2004. Coastal uplift and thrust faulting associated with the $M_w = 6.8$ Zemmouri (Algeria) earthquake of 21 May, 2003. *Geophysical Research Letters*, **31**, L19605, http://dx.doi.org/10.1029/2004GL020466.

MEYSSIGNAC, B. & CAZENAVE, A. 2012. Sea level: a review of present-day and recent-past changes and variability. *Journal of Geodynamics*, **58**, 96–109.

MITROVICA, J. X. & MILNE, G. A. 2003. On post-glacial sea level: 1. General theory. *Geophysical Journal International*, **154**, 253–267.

MORHANGE, C., BOURCIER, M., LABOREL, J., GIALLANELLA, C., GOIRAN, J., CRIMACO, L. & VECCHI, L. 1999. New data on historical relative sea level movements in Pozzuoli, Phlaegrean Fields, southern Italy. *Physics and Chemistry of the Earth*, **24**, 349–354.

MORHANGE, C., LABOREL, J. & HESNARD, A. 2001. Changes of relative sea level during the past 5000

years in the ancient harbour of Marseilles, Southern France. *Palaeogeography, Palaeoclimatology, Palaeoecology*, **166**, 319–329.

Morhange, C., Marriner, N., Laborel, L., Todesco, M. & Oberlin, C. 2006. Rapid sea-level movements and non eruptive crustal deformations in the Phlegrean Fields caldera, Italy. *Geology*, **34**, 93–96.

Mourtzas, N. D. 2012. A palaeogeographic reconstruction of the seafront of the ancient city of Delos in relation to Upper Holocene sea level changes in the central Cyclades. *Quaternary International*, **250**, 3–18.

Nakada, M. & Lambeck, K. 1987. Glacial rebound and relative sea-level variations: a new appraisal. *Geophysical Journal of the Royal Astronomical Society*, **90**, 171–224.

Nocquet, J. M. 2012. Present-day kinematics of the Mediterranean: a comprehensive overview of GPS results. *Tectonophysics*, **579**, 220–242.

Nott, J. 2003. Waves coastal boulders and the importance of the pre-transport setting. *Earth and Planetary Science Letters*, **210**, 296–276.

Pagliarulo, R., Antonioli, F. & Anzidei, M. 2013. Sea level changes since Middle Ages along the coast of Adriatic sea: the case of St. Nicholas Basilica in Bari (Southern Italy). *Quaternary International*, **288**, 139–145.

Pavlopoulos, K. 2010. Relative sealevel fluctuations in Aegean coastal areas from middle to late Holocene. *Geodinamica Acta*, **23**, 5–6.

Pavlopoulos, K., Evelpidiou, N. & Vassilopoulos, A. 2009. *Mapping Geomorphological Environments*. Springer, London.

Peltier, W. R. & Andrews, J. T. 1976. Glacial isostatic adjustment. The forward problem. *Geophysical Journal of the Royal Astronomical Society*, **46**, 605–646.

Pignatelli, C., Sansò, P. & Mastronuzzi, G. 2009. Evaluation of tsunami flooding using geomorphologic evidence. *Marine Geology*, **260**, 6–18.

Pirazzoli, P., Stiros, S. C., Arnold, M., Laborel, J., Laborel-Deguen, F. & Papageorgiou, S. 1994. Episodic uplift deduced from Holocene shorelines in the Perachora Peninsula, Corinth area, Greece. *Tectonophysics*, **229**, 201–209.

Pirazzoli, P. A., Laborel, J. & Stiros, S. C. 1996*a*. Coastal indicators of rapid uplift and subsidence: examples from Crete and other eastern Mediterranean sites. *Zeitschrift für Geomorphologie, N.F. Suppl.-Bd.*, **102**, 21–35.

Pirazzoli, P. A., Laborel, J. & Stiros, S. C. 1996*b*. Earthquake clustering in the eastern Mediterranean during historical times. *Journal of Geophysics Research*, **101**, 6083–6097.

Pirazzoli, P. A., Stiros, S. C., Arnold, M., Laborel, J. & Laborel-Deguen, F. 1999. Late Holocene coseismic vertical displacements and tsunami deposits near Kynos, Gulf of Euboea, Central Greece. *Physics and Chemestry of the Earth*, **24**, 361–367.

Pondrelli, S. 1999. Pattern of seismic deformation in the Western Mediterranean. *Annals of Geophysics*, **42**, 57–70.

Pondrelli, S., Morelli, A. & Boschi, E. 1995. Seismic deformation in the Mediterranean area estimated by moment tensor summation. *Geophysical Journal International*, **122**, 938–952.

Pondrelli, S., Morelli, A. & Ekström, G. 2004. European–Mediterranean regional centroid moment tensor catalogue: solutions for years 2001–2002. *Physics of the Earth Planetary Interior*, **145**, 127–147.

Pondrelli, S., Salimbeni, S., Ekström, G., Morelli, A., Gasperini, P. & Vannucci, G. 2006. The Italian CMT dataset from 1977 to the present. *Physics of the Earth Planetary Interior*, **159**, 286–303.

Pondrelli, S., Salimbeni, S., Morelli, A., Ekström, G. & Boschi, E. 2007. European–Mediterranean regional centroid moment tensor catalogue: solutions for years 2003–2004. *Physics of the Earth Planetary Interior*, **164**, 90–112.

PROCOPE DE CÉSARÉE 1962. *History of the Wars Buildings: The Gothic war, Books 6–7*. Heinemann Limited–Harvard University Press, Cambridge, MA.

Rahmstorf, S., Cazenave, A., Church, J. A., Hansen, J. E., Keeling, R. F., Parker, D. E. & Somerville, R. C. J. 2007. Recent climate observations compared to projections. *Science*, **316**, 709.

Rebai, S., Philip, H. & Taboada, A. 1992. Modern tectonic stress field in the Mediterranean region: evidence for variation in stress directions at different scale. *Geophysical Journal International*, **110**, 106–140.

Renfrew, C. & Aspinall, A. 1990. Aegean obsidian and Franchthi Cave. *In*: Perles, C. (ed.) *Les industries lithiques taillées de Franchthi (Argolide, Grèce) Tome II. Les industries du Mésolithique et du Néolithique Initial*. Indiana University Press, Bloomington, 257–270.

Ridente, D., Fracassi, U., Di Bucci, D., Trincardi, F. & Valensise, G. 2008. Middle Pleistocene to Holocene activity of the Gondola fault zone (Southern Adriatic foreland): deformation of a regional shear zone and seismotectonic implications. *Tectonophysics*, **453**, 110–121.

Roberts, G. P., Houghton, S. L. *et al.* 2009. Localization of Quaternary slip rates in an active rift in 105 years: an example from central Greece constrained by ^{234}U-^{230}Th coral dates from uplifted paleoshorelines. *Journal of Geophysical Research*, **114**, B10406, http://dx.doi.org/10.1029/2008JB005818

Rodriguez-Vidal, J., Caceres, L. M., Finlayson, J. C., Garcia, F. J. & Martinez-Aguirre, A. 2004. Neotectonics and shoreline history of the Rock of Gibraltar, southern Iberia. *Quaternary Science Reviews*, **23**, 2017–29.

Romagnoli, C. 2013. Characteristics and morphological evolution of the Aeolian volcanoes from the study of submarine portions. *In*: Lucchi, F., Peccerillo, A., Keller, J., Tranne, C. A. & Rossi, P. L. (eds) *The Aeolian Islands Volcanoes*. The Geological Society, London, Memoirs, **37**, 13–26.

Rovere, A., Vacchi, M., Firpo, M. & Carobene, L. 2011. Underwater geomorphology of the rocky coastal tracts between Finale Ligure and Vado Ligure (western Liguria, NW Mediterranean Sea). *Quaternary International*, **232**, 187–200.

Rovere, A., Furlani, S., Benjamin, J., Fontana, A. & Antonioli, F. 2012. MEDFLOOD project: MEDiterranean sea-level change and projection for future

FLOODing. *Alpine and Mediterranean Quaternary*, **25**, 3–5.

Rueda, J. & Mezcua, J. 2005. Near-real-time seismic moment-tensor determination in Spain. *Seismological Research Letters*, **76**, 455–465.

Scheffers, A. & Scheffers, S. 2007. First significant tsunami evidence from historical times in western Crete (Greece). *Earth and Planetary Letters*, **259**, 613–624.

Scheffers, A., Kelletat, D., Vött, A., May, M. & Scheffers, S. 2008. Late holocene tsunami traces on the western and southern coastlines of the Peloponnesus (Greece). *Earth and Planetary Science Letters*, **269**, 271–279.

Schmiedt, G., Caputo, M., Conta, G., Guidi, F., Pellegrini, M. & Pieri, L. 1972. *Il livello antico del mar Tirreno. Testimonianze dei resti archeologici*. Olschki, Firenze, 326 pp.

Scognamiglio, L., Tinti, E. & Michelini, A. 2009. Real-time determination of seismic moment tensor for the Italian region. *Bulletin of the Seismological Society of America*, **99**, 2223–2242, http://dx.doi.org/10.1785/0120080104

Serpelloni, E., Anzidei, M., Baldi, P., Casula, G., Galvani, A., Pesci, A. & Riguzzi, F. 2002. Combination of permanent and non-permanent GPS networks for the evaluation of the strain-rate field in the central Mediterranean area. *Bollettino di Geofisica Teorica ed Applicata*, **43**, 195–219.

Serpelloni, E., Anzidei, M., Baldi, P., Casula, G. & Galvani, A. 2005. Crustal velocity and strain-rate fields in Italy and surrounding regions: new results from the analysis of permanent and non-permanent GPS networks. *Geophysical Journal International*, **161**, 861–880, http://dx.doi.org/10.1111/j.1365–246X.2005.02618.x

Serpelloni, E., Anzidei, M., Baldi, P., Casula, G. & Galvani, A. 2006. GPS measurement of active strains across the Apennines. *Annals of Geophysics*, **49**, 319–329.

Serpelloni, E., Vannucci, G. *et al*. 2007. Kinematics of the Western Africa–Eurasia plate boundary from focal mechanisms and GPS data. *Geophysical Journal International*, **169**, 1180–1200.

Serpelloni, E., Bürgmann, R., Anzidei, M., Baldi, P., Mastrolembo Ventura, B. & Boschi, E. 2010. Strain accumulation across the Messina Straits and kinematics of Sicily and Calabria from GPS data and dislocation modelling. *Earth and Planetary Science Letters*, **298**, 347–360.

Serpelloni, S., Faccenna, C., Spada, G., Dong, D. & Williams, S. D. P. 2013. Vertical GPS ground motion rates in the Euro-Mediterranean region: new evidence of velocity gradients at different spatial scales along the Nubia–Eurasia plate boundary. *Journal of Geophysical Research*, **118**, 1–22. http://dx.doi.org/10.1002/2013JB010102

Shah-Hosseini, M., De Marco, A. *et al*. 2013. Coastal boulders in Martigues, French Mediterranean: evidence for extreme storm waves during the Little Ice Age. *Zeitschrift für Geomorphologie*, **57**(Suppl 4), http://dx.doi.org/10.1127/0372-8854/2013/S-00132

Shaw, B., Ambraseys, N. N. *et al*. 2008. Eastern Mediterranean tectonics and tsunami hazard inferred from the AD 365 earthquake. *Nature Geosciences*, **1**, 268–276.

Shiki, T., Tachibana, T., Fujiwara, O., Goto, K., Nanayama, F. & Yamazaki, T. 2008. Characteristic Features of tsunamiites. *In*: Shiki, T., Tsuji, Y., Yamasaki, T. & Minoura, K. (eds) *Tsunamiites. Features and Implications*. Elsevier, New York, 319–340.

Sivan, D., Lambeck, K., Galili, E. & Raban, A. 2001. Holocene sea-level changes along the Mediterranean coast of Israel, based on archaeological observations and numerical model. *Palaeogeography, Palaeoclimatology, Palaeoecology*, **167**, 101–117.

Sivan, D., Lambeck, K., Toueg, R., Raban, A., Porath, Y. & Shirman, B. 2004. Ancient coastal wells of Caesarea Maritima, Israel, an indicator for sea level changes during the last 2000 years. *Earth and Planetary Science Letters*, **222**, 315–330.

Slim, H., Trusset, P., Paskoff, R. & Oueslati, A. 2004. *Le littoral de la Tunisie*. CNRS Editions, Paris, Etude Géoarchéologique et Historique, Etudes d'Antiquités africaines for Libyan Studies, **36**, 1–308.

Soloviev, S. L., Solovieva, O. N., Go, C. N., Kim, K. S. & Shchetnikov, N. A. 2000. *Tsunami in the Mediterranean Sea 2000 B.C.–2000 A.D*. Advances in Natural and Technological Hazards Research, Kluwer Academic, Dordrecht.

Spencer, T. 1988. Coastal biogeomorphology. *In*: Viles, H. A. (ed.) *Biogeomorphology*. Basil Blackwell, New York, 255–318.

Stich, D., Serpelloni, E., Mancilla, F. & Morales, J. 2006. Kinematics of the Iberia–Maghreb plate contact from seismic moment tensors and GPS observations. *Tectonophysics*, **426**, 295–317.

Stiros, S. C. 2001. The AD 365 Crete earthquake and possible seismic clustering during the fourth to sixth centuries AD in the Eastern Mediterranean: a review of historical and archaeological data. *Journal of Structural Geology*, **23**, 545–562.

Stiros, S. C. 2010. The 8.5+ magnitude, AD 365 earthquake in Crete: coastal uplift, topography changes, archaeological and historical signature. *Quaternary International*, **216**, 54–63.

Sunamura, T. 1992. *Geomorphology of Rocky Coasts*. John Wiley, Chichester.

Tallarico, A., Dragoni, M., Anzidei, M. & Esposito, A. 2003. Modeling long-term ground deformation due to the cooling of a magma chamber: case of Basiluzzo island, Aeolian Islands, Italy. *Journal of Geophysical Research*, **108**, 2568, http://dx.doi.org/10.1029/2002JB002376

Tinti, S. & Armigliato, A. 2003. The use of scenarios to evaluate tsunami impact in South Italy. *Marine Geology*, **199**, 221–243.

Tinti, S., Maramai, A. & Graziani, L. 2007. The Italian Tsunami Catalogue (ITC), http://www.ingv.it/servizi-erisorse/BD/catalogo-tsunami/catalogo-degli-tsunami-italiani

Toker, E., Sivan, D., Stern, E., Shirman, B., Tsimplis, M. & Spada, G. 2011. Evidence for centennial scale sea level variability during the Medieval Climate Optimum (Crusader Period) in Israel, eastern Mediterranean. *Earth and Planetary Science Letters*, **315–316**, 51–61, http://dx.doi.org/10.1016/j.epsl.2011.07.019

ULUG, A., DUMAN, M., ERSOY, S., OZEL, E. & AVCI, M. 2005. Late Quaternary sea-level change, sedimentation and neotectonics of the Gulf of Gokova, southeastern Aegean Sea. *Marine Geology*, **221**, 381–395.

VACCHI, M., ROVERE, A., ZOUROS, N. & FIRPO, M. 2012*a*. Assessing enigmatic boulder deposits in NE Aegean Sea: importance of historical sources as tool to support hydrodynamic equations. *Natural Hazards Earth System Science*, **12**, 1109–1118.

VACCHI, M., ROVERE, A., ZOUROS, N., DESRUELLES, S., CARON, V. & FIRPO, M. 2012*b*. Spatial distribution of sea-level markers on Lesvos Island (NE Aegean Sea): evidence of differential relative sea-level changes and the neotectonic implications. *Geomorphology*, **159–160**, 50–62. http://dx.doi.org/10.1016/j.geomorph.2012.03.004

VAN ANDEL, T. H. 1989. Late Quaternary sea-level changes and archaeology. *Antiquity*, **63**, 733–46.

VANNUCCI, G. & GASPERINI, P. 2004. The new release of the database of Earthquake Mechanisms of the Mediterranean Area (EMMA Version 2). *Annals of Geophysics*, **47**, 307–334.

VANNUCCI, G., PONDRELLI, S., ARGNANI, A., MORELLI, A., GASPERINI, P. & BOSCHI, E. 2004. An Atlas of Mediterranean seismicity. *Annals of Geophysics*, **47**, 247–306.

VECCHIO, A., ANZIDEI, M., CAPPARELLI, V., CARBONE, V. & GUERRA, I. 2012. Has the Mediterranean Sea felt the March 11th, 2011, Mw 9.0 Tohoku–Oki earthquake? *Europhysics Letters*, **98**, 1–6.

VELLA, C., DEMORY, F., CANUT, V., DUSSOUILLEZ, P. & FLEURY, T. J. 2011. First evidence of accumulation of mega boulders on the Mediterranean rocky coast of Provence (southern France). *Natural Hazards and Earth System Sciences*, **11**, 905–914.

VÖTT, A., BARETH, G. *ET AL*. 2010. Beachrock-type calcarenitic tsunamites along the shores of the eastern Ionian Sea (western Greece) – case studies from Akarnania, the Ionian Islands and the western Peloponnese. *Zeitschrift für Geomorphologie*, **54**(suppl. 3), 1–50.

WDOWINSKI, S., BOCK, Y., ZHANG, J., FANG, P. & GENRICH, J. 1997. Southern California Permanent GPS Geodetic Array: spatial filtering of daily positions for estimating coseismic and postseismic displacements induced by the 1992 Landers earthquake. *Journal of Geophysical Research*, **102**, 18057–18070.

WESTAWAY, R. 1990. Present-day kinematics of the plate boundary zone between Africa and Europe, from the Azores to the Aegean. *Earth Planetary Science Letters*, **96**, 393–406.

WESTAWAY, R. 1992. Seismic moment summation for historical earthquakes in Italy: tectonic implications. *Journal of Geophysical Research*, **97**, 437–15464.

WHELAN, F. & KELLETAT, D. 2002. Geomorphic evidence and relative and absolute dating results for tsunami events on Cyprus. *Science of Tsunami Hazards*, **20**, 3–18.

WÖPPELMANN, G. & MARCOS, M. 2012. Coastal sea level rise in southern Europe and the non-climate contribution of vertical land motion. *Journal of Geophysical Research*, **117**, C01007, http://dx.doi.org/10.1029/2011JC007469

ZAZO, C., SILVA, P. G. *ET AL*. 1999. Coastal uplift in continental collision plate boundaries: data from the Last Interglacial marine terrace of the Gibraltar Straits area (south Spain). *Tectonophysics*, **301**, 95–109.